

Effective Field Theory and Time-Reversal Violation in Light Nuclei

E. Mereghetti¹ and U. van Kolck^{2,3}

¹*Theoretical Division, Los Alamos National Laboratory,
Los Alamos, NM 87545, USA*

²*Institut de Physique Nucléaire, CNRS/IN2P3, Université Paris Sud,
91406 Orsay, France*

³*Department of Physics, University of Arizona,
Tucson, AZ 85721, USA*

Accepted for publication in *Ann. Rev. Nucl. Part. Sci.* **65** (2015)

Abstract

Thanks to the unnaturally small value of the QCD vacuum angle $\bar{\theta} \lesssim 10^{-10}$, time-reversal violation (\mathcal{T}) offers a window into physics beyond the Standard Model (SM) of particle physics. We review the effective-field-theory framework that establishes a clean connection between \mathcal{T} mechanisms, which can be represented by higher-dimensional operators involving SM fields and symmetries, and hadronic interactions, which allow for controlled calculations of low-energy observables involving strong interactions. The chiral properties of \mathcal{T} mechanisms leads to a pattern that should be identifiable in measurements of the electric dipole moments of the nucleon and light nuclei.

Contents

1	Introduction	1
2	\mathcal{T} at the Quark-Gluon Level	4
2.1	QCD $\bar{\theta}$ Term and Higher-Dimensional Operators	4
2.2	Sizes and Runnings of \mathcal{T} Couplings	7
3	\mathcal{T} at the Hadronic Level	10
3.1	Chiral Symmetry and Low-Energy Interactions	10
3.2	Sizes of \mathcal{T} Couplings	12
4	Peccei-Quinn Mechanism	15
5	Nucleon Electric Dipole Moment	16
5.1	Chiral EFT	16
5.2	Interplay with Lattice QCD	18
5.3	Role of Strangeness	20
6	\mathcal{T} Moments of Light Nuclei	22
6.1	Nuclear Potential and Currents	22
6.2	Moments	24
7	Outlook	27

1 Introduction

Violation of time reversal (T) is a fundamental asymmetry between past and future, the microscopic dynamics not being invariant under change in the sign of time. In a Lorentz-invariant quantum field theory, where the product CPT is conserved, T violation (\mathcal{T}) is equivalent to violation of the product of charge conjugation (C) —the exchange between particle and antiparticle— and parity (P) —the change of sign in spatial coordinates. CP violation (\mathcal{CP}) is one of the ingredients [1] needed to explain why the visible universe seems to be made predominantly of matter, without a significant fraction of antimatter [2].

The Standard Model (SM) [3, 4] contains a source of \mathcal{CP} and \mathcal{T} : the phase of the CKM matrix [5], which appears in observables through a combination $J \simeq 3 \cdot 10^{-5}$ of matrix elements [6]. While this mechanism explains the violation observed in K and B decays [7], it gives only very small contributions to quantities that do not involve flavor change between initial and final states. In particular, it is not sufficiently large to account for the observed matter-antimatter asymmetry [8].

The ideal observables to probe new \mathcal{T} interactions are flavor-conserving observables such as \mathcal{T} electromagnetic form factors (FFs), which can be split into electric, magnetic, and toroidal, depending on whether they interact with long-range electric, long-range magnetic, or short-range electromagnetic fields. Their P and T transformation properties are summarized in

Multipolarity	Electric	Magnetic	Toroidal
0 (monopole)	PT	—	—
1 (dipole)	$\cancel{P}\cancel{\mathcal{I}}$	PT	$\cancel{P}T$
2 (quadrupole)	PT	$\cancel{P}\cancel{\mathcal{I}}$	$P\cancel{\mathcal{I}}$
...

Table 1: Parity and time-reversal properties of electromagnetic form factors according to multipolarity. S (\cancel{S}) denotes that the symmetry S is preserved (violated). The pattern repeats as multipolarity increases. A particle of spin s has multipoles up to $2s$.

Table 1. Of particular interest are permanent electric dipole moments (EDMs), which require both \cancel{P} and $\cancel{\mathcal{I}}$. Even with current technology they effectively probe very small distances. For example, the existing bound on the neutron EDM, $|d_n| < 2.9 \cdot 10^{-13} e \text{ fm}$ [9], means that a charge imbalance, if any, effectively takes place at a distance 13 (or more) orders of magnitude smaller than the size of the neutron. Other $\cancel{\mathcal{I}}$ multipoles, like magnetic (MQM) and toroidal (TQM) quadrupole moments, are less accessible experimentally.

Searches are in progress around the world for EDMs of the neutron and of (neutral) atoms and molecules, which are sensitive to the EDMs of the electron and nuclei, and their $\cancel{\mathcal{I}}$ interactions. A new generation of experiments [10] promises to improve neutron EDM sensitivity by one or two orders of magnitude, which is remarkable but still above the expected CKM “background” at $\sim 10^{-19} e \text{ fm}$ (see Ref. [11] for an assessment and references to original papers, and Ref. [12] for a recent discussion). Even more exciting is the groundbreaking proposal (see Refs. [13,14] for summaries and references) that the EDMs of charged particles be investigated in specifically designed storage rings, and not just as byproducts of other experiments as for the muon [15]. We might see the deuteron EDM (d_d) probed at the level of $\sim 10^{-16} e \text{ fm}$ [14], and similarly for the EDMs of the proton (d_p) and of the nucleus of helium-3, helion (d_h).

The discovery of an EDM above the CKM background would be a signal of long-sought new physics, but would, by itself, leave us in the dark about its origins. From a theoretical perspective, it is important to investigate the set of EDMs that would allow us to identify the dominant source(s) of $\cancel{\mathcal{I}}$. Such an identification is likely to give clues about physics beyond the SM (BSM) and the scale of this new physics, which we denote M_T . The aim of this review is to show that the framework of effective field theories (EFTs), coupled to recent and not-too-distant-future progress in strong-interaction physics, will allow us to carry out this identification for the $\cancel{\mathcal{I}}$ operators that involve quarks and gluons.

There are good experimental and theoretical reasons to believe that the SM is an EFT for processes involving momenta $Q \sim M_{\text{EW}} \sim 100 \text{ GeV}$. In addition to the possible existence of new light or stable heavy particles, new physics can be represented at the electroweak (EW) scale M_{EW} by operators of canonical dimensions $d > 4$, which involve known particles and are constrained by the SM symmetries, namely Lorentz invariance and gauged $SU(3)_c \times SU(2)_L \times U(1)_Y$. One expects these operators to have strengths $\mathcal{O}(M_T^{4-d})$, making the lowest-dimension operators most significant.

The SM has other $d = 4$ $\cancel{\mathcal{I}}$ operators, which involve the non-Abelian gauge bosons and, despite being total derivatives, can contribute to $\cancel{\mathcal{O}}\mathcal{P}$ observables due to topological effects

[16]. The operator involving gluons could give rise to large EDMs of hadrons and nuclei, but the neutron EDM bound already significantly constrains its dimensionless strength, the QCD vacuum angle $\bar{\theta} \lesssim 10^{-10}$. This unnatural value is the famous “strong CP problem”. The most promising solution is offered by the Peccei-Quinn (PQ) mechanism [17], where an additional approximate symmetry, $U(1)_{PQ}$, is spontaneously broken generating a small $\bar{\theta}$ dynamically. The corresponding pseudo-Goldstone boson, the axion [18, 19], is a viable dark-matter candidate. Whatever the mechanism may be, the smallness of $\bar{\theta}$ leaves room for higher-dimensional operators.

The sole $d = 5$ interaction among known particles [20] gives rise to neutrino masses and lepton-number violating processes, which are searched for with neutrinoless double-beta decay (see Ref. [21] for a recent review). One can expect \mathcal{CP} violation from phases in the corresponding PMNS mixing matrix [22], but it is unclear if the observed baryon-antibaryon asymmetry can be generated through leptogenesis [23], a mechanism based on the simplest ultraviolet (UV) completion of the $d = 5$ interaction.

The many $d = 6$ interactions [24] have been conveniently cataloged in Ref. [25]. Among those responsible for \mathcal{CP} [26], hadronic and nuclear EDMs are most sensitive to quark EDMs (qEDMs) and chromo-EDMs (qCEDMs), the gluon chromo-EDM (gCEDM) [27], and certain four-quark interactions [28, 29]. Nowadays the techniques exist —renormalization-group (RG) running down to the QCD scale $M_{\text{QCD}} \sim 1$ GeV, lattice QCD (LQCD) for the calculation of low-energy constants (LECs), nuclear EFTs to describe the dynamics at momenta $Q < M_{\text{QCD}}$ in terms of the LECs— to connect these operators at the EW scale to light-nuclear EDMs.

A frequent misconception is that nuclear-physics errors would obfuscate any of the minute \mathcal{F} effects we are interested in. This presumption is obviously not correct for quantities like EDMs, which vanish when \mathcal{F} parameters vanish; in this case errors affect only the proportionality factor, and as we are going to see they should not affect many of the conclusions. Light nuclei are special in this regard. A key ingredient is the approximate chiral symmetry of QCD, and its breaking. Not only does chiral symmetry provide the basis for a systematic expansion of hadronic and nuclear observables in powers of Q/M_{QCD} [30], but it also acts as a “filter” to separate the effects of various \mathcal{F} sources. While all these sources generate \mathcal{F} observables, they break chiral symmetry in different ways and as a consequence produce different patterns in the relative magnitudes for these observables. Chiral symmetry was already an important aspect of the classic studies of the neutron EDM from $\bar{\theta}$ [31, 32], and now it has been extended to other sources and more nucleons [33–36]. A single measurement (say, d_n) can always be attributed to any one source (say, a $\bar{\theta}$ of just the right, minute size), but, as we review in Sections 5 and 6, combined measurements of d_n , d_p , d_d and d_h provide increasingly detailed information on the \mathcal{F} sources. The further measurement of the triton EDM (d_t) would allow as good a separation of underlying mechanisms as possible in the strong-interacting sector at low energies, under the assumption that lower-dimension operators are most important. (Measurements of the deuteron MQM and TQM would also be valuable, but seem impossible for the foreseeable future.)

All the main techniques needed for this analysis have experienced significant progress recently. RG running down to the QCD scale has long been used as a tool to investigate the low-energy consequences of specific BSM models, and a model-independent summary of these results has appeared recently [37]. Computational advances are bringing LQCD to the forefront

of hadronic and nuclear physics, and the time is approaching when EFTs will be able to use LQCD data, rather than experiment, as input in the calculation of nuclear properties [38]. Still, the study of \mathcal{Z} matrix elements is in its infancy, particularly for $d > 4$ operators, and this constitutes the biggest gap in connecting nucleon and light-nuclear EDMs to BSM \mathcal{Z} interactions. Nuclear EFTs [30] make it possible to approach hadronic and nuclear physics incorporating SM symmetries, and the \mathcal{Z} hadronic interactions involve, in lowest order, six LECs. Nuclear potentials inspired by Chiral EFT [39, 40], where pions and chiral symmetry play a significant role, are now the favorite starting point for “*ab initio*” nuclear-structure methods. Although fully consistent calculations are not yet possible, for light nuclei several tests suggest that errors are relatively small and can be better quantified once some subtleties in the RG of pion exchange are clarified [41, 42]. A significant future step would be to extend the framework summarized here to heavier nuclei, in order to enable a consistent analysis of atomic/molecular experiments as well.

We limit ourselves here to a review of the techniques that address \mathcal{Z} in the nucleon and light nuclei from a model-independent perspective. The relevant operators at the quark/gluon level, including the RG to M_{QCD} , are introduced in Section 2 and translated into hadronic interactions in Section 3. The PQ mechanism is briefly summarized in Section 4. Sections 5 and 6 review calculations of \mathcal{Z} electromagnetic observables for the nucleon and light nuclei, respectively, starting from the hadronic interactions. An outlook is reserved for Section 7. A much more comprehensive review—which includes implications of specific BSM models, calculations of QCD matrix elements with various assumptions, calculations of heavy-nuclear \mathcal{Z} quantities, a discussion of atomic/molecular EDMs, and many more references to earlier work—has appeared recently [43], and we refer the reader to it for a more detailed look at how the program presented here relates to other efforts.

2 \mathcal{Z} at the Quark-Gluon Level

We summarize here the most important \mathcal{Z} interactions among quarks, gluons and photons. This background will allow the construction of \mathcal{Z} hadronic interactions in Section 3.

2.1 QCD $\bar{\theta}$ Term and Higher-Dimensional Operators

BSM physics can be described below its characteristic scale $M_T > M_{\text{EW}}$ in terms of $SU(3)_c \times SU(2)_L \times U(1)_Y$ and Lorentz-symmetric operators. The kinetic terms involving quarks interacting with gluons G_μ^a ($a = 1, \dots, 8$) and weak bosons W_μ^i ($i = 1, 2, 3$) and B_μ with strengths g_s , g , and g' , respectively, are

$$\mathcal{L}_T^{(4)} = \bar{q}_L i \not{D} q_L + \bar{u}_R i \not{D} u_R + \bar{d}_R i \not{D} d_R - \frac{1}{4} (G_{\mu\nu}^a G^{a\mu\nu} + W_{\mu\nu}^i W^{i\mu\nu} + B_{\mu\nu} B^{\mu\nu}), \quad (1)$$

where q_L is a doublet of left-handed quarks; u_R and d_R are right-handed up- and down-type quarks; $D_\mu = \partial_\mu - ig_s G_\mu^a t_a - ig W_\mu^i t_i - ig' B_\mu Y$ is the gauge covariant derivative with $t_a = \lambda_a/2$ (λ_a are the Gell-Mann matrices), $t_i = \tau_i/2, 0, 0$ (τ_i are the Pauli matrices) and $Y = 1/6, 2/3, -1/3$ for q_L , u_R and d_R , respectively; and $G_{\mu\nu}^a = \partial_\mu G_\nu^a - \partial_\nu G_\mu^a - g_s f^{abc} G_\mu^b G_\nu^c$,

$W_{\mu\nu}^i = \partial_\mu W_\nu^i - \partial_\nu W_\mu^i - g\epsilon^{ijk}W_\mu^jW_\nu^k$, and $B_{\mu\nu} = \partial_\mu B_\nu - \partial_\nu B_\mu$ are, respectively, the $SU(3)_c$, $SU(2)_L$, and $U(1)_Y$ field strengths with structure constants f^{abc} for $SU(3)_c$ and ϵ^{ijk} for $SU(2)_L$. For simplicity we omit indices that run through the three generations, which are summed over.

The $d = 4$ terms related to \mathcal{F} are the Yukawa couplings of the quarks and the topological θ term [16],

$$\mathcal{L}_T^{(4)} = -(\bar{q}_L Y^u \tilde{\varphi} u_R + \bar{q}_L Y^d \varphi d_R) + \text{H.c.} - \theta \frac{g_s^2}{64\pi^2} \epsilon^{\mu\nu\alpha\beta} G_{\mu\nu}^a G_{\alpha\beta}^a, \quad (2)$$

where φ is the Higgs doublet and $\tilde{\varphi}^I = \epsilon^{IJ}\varphi^{J*}$. (Here $\epsilon^{01} = \epsilon^{012} = \epsilon^{0123} = +1$.) The Yukawa couplings $Y^{u,d}$ form 3×3 complex matrices in flavor space. Relative phases lead to \mathcal{CP} in the CKM matrix [5] and, as described below, there is an interplay between the overall phase and the vacuum angle $0 \leq \theta < 2\pi$. A term analogous to θ for weak gauge bosons gives negligible contributions at low energies.

Because of the smallness of $d = 4$ \mathcal{F} , we follow Refs. [35, 36] and consider the $d = 6$ terms [25],

$$\begin{aligned} \mathcal{L}_T^{(6)} = & -2\frac{\varphi^\dagger\varphi}{v^2} \left[(\bar{q}_L Y'^u \tilde{\varphi} u_R + \bar{q}_L Y'^d \varphi d_R) + \text{H.c.} + \theta' \frac{g_s^2}{64\pi^2} \epsilon^{\mu\nu\alpha\beta} G_{\mu\nu}^a G_{\alpha\beta}^a \right] \\ & - \frac{1}{\sqrt{2}} \bar{q}_L \sigma^{\mu\nu} \left(g_s \tilde{\Gamma}^u t_a G_{\mu\nu}^a + g \Gamma_{W\tau_i}^u W_{\mu\nu}^i + g' \Gamma_B^u B_{\mu\nu} \right) \tilde{\varphi} u_R + \text{H.c.} \\ & - \frac{1}{\sqrt{2}} \bar{q}_L \sigma^{\mu\nu} \left(g_s \tilde{\Gamma}^d t_a G_{\mu\nu}^a + g \Gamma_{W\tau_i}^d W_{\mu\nu}^i + g' \Gamma_B^d B_{\mu\nu} \right) \varphi d_R + \text{H.c.} \\ & + \frac{d_W}{6} g_s f^{abc} \epsilon^{\mu\nu\alpha\beta} G_{\alpha\beta}^a G_{\mu\rho}^b G_\nu^{c\rho} + g_s^2 \bar{u}_R \Xi_1 \gamma^\mu d_R \tilde{\varphi}^\dagger i D_\mu \varphi + \text{H.c.} \\ & + g_s^2 \epsilon^{JK} [\Sigma_1 \bar{q}_L^J u_R \bar{q}_L^K d_R + \Sigma_8 \bar{q}_L^J t_a u_R \bar{q}_L^K t_a d_R] + \text{H.c.}, \end{aligned} \quad (3)$$

where $v \simeq 246$ GeV is the Higgs vacuum expectation value (vev). Here:

- The 3×3 complex matrices $Y'^{u,d}$ and the angle θ' correct, after EW symmetry breaking, Yukawa couplings and θ term. Terms linear in the Higgs field are of more phenomenological interest, as they either modify the Yukawa couplings of the Higgs to quarks introducing, in general, flavor-changing effects, or affect the gluon-fusion production mechanism at the LHC [44–47].
- The coefficients $\tilde{\Gamma}^{u,d}$ and $\Gamma_{B,W}^{u,d}$ are 3×3 matrices in flavor space. The nondiagonal entries contribute to flavor-changing currents and play an important role in flavor physics [48, 49]. The diagonal components determine the quark electric (qEDM) and chromoelectric (qCEDM) dipole moments, as well as the quark weak EDM, which plays only a minor role at low energy.
- The parameter d_W of the Weinberg three-gluon operator [27] can be thought of as the gluon chromoelectric dipole moment (gCEDM). Similar terms involving weak gauge bosons (for example, the W^\pm boson's EDM and MQM [50]) can be relevant at colliders, but are very small at energies below M_{EW} .

- The $\Sigma_{1,8}$ are complex four-index tensors in flavor space. If one considers only quarks of the first generation, there are two \mathcal{CP} four-quark operators that respect $SU(2)_L$ [28], which we refer to as PS4QOs due to their pseudoscalar nature. Additional four-quark operators can be constructed involving quarks of different generations.
- The complex 3×3 matrix Ξ_1 couples W^\pm bosons to the right-handed quark current. It leads below M_{EW} to additional \mathcal{CP} four-quark operators [29], which couple left- and right-handed quarks and we call LR4QOs. It also causes \mathcal{CP} in nuclear β decay when W^\pm connect to the left-handed lepton current [29].

The $d = 6$ coefficients depend on the spectrum and \mathcal{CP} parameters of the BSM model of choice, and can be determined by matching just below the scale M_T . While a detailed study is beyond the scope of this review (see instead Ref. [43]), from our brief discussion it is apparent that there is a rich interplay among the constraints on the couplings in Eq. (3) that can be extracted from collider, flavor, and low-energy precision experiments.

Below the scale M_{EW} the breaking of $SU(3)_c \times SU(2)_L \times U(1)_Y$ to $SU(3)_c \times U(1)_{em}$ is important and generates masses for fermions and weak gauge bosons. For studying low-energy observables like EDMs, the Lagrangian (3) at the EW scale needs to be matched onto a theory with only light quarks, gluons and the photon $A_\mu = \sin \theta_W W_\mu^3 + \cos \theta_W B_\mu$, where $g \sin \theta_W = g' \cos \theta_W = -e < 0$. For nuclear physics applications we can limit ourselves to two light flavors, and at M_{QCD} the kinetic terms can be written as

$$\mathcal{L}_T^{(4)} = \bar{q}_L i \not{D} q_L + \bar{q}_R i \not{D} q_R - \frac{1}{4} G_{\mu\nu}^a G^{a\mu\nu} - \frac{1}{4} F_{\mu\nu} F^{\mu\nu}, \quad (4)$$

where $q = (u \ d)^T$, $D_\mu = \partial_\mu - ig G_\mu^a t_a - ie A_\mu Q$ is the $SU(3)_c \times U(1)_{em}$ covariant derivative in terms of the charge matrix $Q = 1/6 + \tau_3/2$, and $F_{\mu\nu} = \partial_\mu A_\nu - \partial_\nu A_\mu$ is the $U(1)_{em}$ field strength. Some of the issues associated with strangeness are discussed in Section 5.3.

\mathcal{CP} from the QCD θ term is intimately related to the quark masses. All the phases of the quark mass matrix can be eliminated through non-anomalous $SU(2)$ vector and axial rotations, except for a common phase ρ , leaving

$$\mathcal{L}_T^{(4)} = - (e^{i\rho} \bar{q}_L M q_R + e^{-i\rho} \bar{q}_R M q_L) - \theta \frac{g_s^2}{64\pi^2} \epsilon^{\mu\nu\alpha\beta} G_{\mu\nu}^a G_{\alpha\beta}^a, \quad (5)$$

where $M = \bar{m}(1 - \varepsilon\tau_3)$ is the diagonal quark mass matrix with \bar{m} (the average light-quark mass) and ε (the relative light-quark mass splitting) real parameters. The phase ρ and the θ angle are not independent. By performing an anomalous axial $U(1)_A$ rotation, all \mathcal{CP} can be rotated into the θ term or into the complex mass term, and physical observables depend only on the combination $\bar{\theta} = \theta + 2\rho$. For our discussion in Chiral EFT, it is convenient to eliminate the θ term in favor of a complex quark mass. The additional $SU(2)$ approximate symmetry of the Lagrangian can be exploited to align the vacuum in the presence of \mathcal{CP} to the usual QCD vacuum [31, 32]. From a low-energy point of view, vacuum alignment is equivalent to setting to zero the coupling of the neutral pion to the vacuum, at lowest order in the Chiral EFT expansion [33]. The Lagrangian becomes

$$\mathcal{L}_T^{(4)} = -\bar{m} r(\bar{\theta}) \bar{q} q + \bar{m} r^{-1}(\bar{\theta}) \bar{q} \left(\varepsilon \tau_3 + \frac{1 - \varepsilon^2}{2} \sin \bar{\theta} i\gamma_5 \right) q, \quad (6)$$

where $r(x)$ is an even function of x ,

$$r(x) = \sqrt{\frac{1 + \varepsilon^2 \tan^2 \frac{x}{2}}{1 + \tan^2 \frac{x}{2}}} = 1 - (1 - \varepsilon^2) \frac{x^2}{8} + \mathcal{O}(x^4). \quad (7)$$

The $\mathcal{O}(\bar{\theta}^2)$ terms become important in the PQ mechanism (Section 4). The last term in Eq. (6) is approximately linear in $\bar{\theta}$, and responsible for \mathcal{CP} .

In the absence of flavor change, the $d = 6$ \mathcal{X} operators that receive tree-level contributions and are not suppressed by powers of M_{EW} are [35]

$$\begin{aligned} \mathcal{L}_T^{(6)} = & -\frac{\bar{m}}{2} \bar{q} \left(d_0 Q + \frac{d_3}{2} \{Q, \tau_3\} \right) i\sigma^{\mu\nu} \gamma_5 q e F_{\mu\nu} - \frac{\bar{m}}{2} \bar{q} \left(\tilde{d}_0 + \tilde{d}_3 \tau_3 \right) i\sigma^{\mu\nu} \gamma_5 t_a q g_s G_{\mu\nu}^a \\ & + \frac{d_W}{6} g_s f^{abc} \epsilon^{\mu\nu\alpha\beta} G_{\alpha\beta}^a G_{\mu\rho}^b G_\nu^{c\rho} \\ & + \frac{g_s^2}{4} [\text{Im}\Sigma_1 (\bar{q}q \bar{q}i\gamma_5 q - \bar{q}\boldsymbol{\tau}q \cdot \bar{q}\boldsymbol{\tau}i\gamma_5 q) + \text{Im}\Sigma_8 (\bar{q}t_a q \bar{q}i\gamma_5 t_a q - \bar{q}\boldsymbol{\tau}t_a q \cdot \bar{q}\boldsymbol{\tau}i\gamma_5 t_a q)] \\ & + \frac{g_s^2}{4} \epsilon^{3ij} (\text{Im}\Xi_1 \bar{q}\tau_i \gamma^\mu q \bar{q}\tau_j \gamma_\mu \gamma_5 q + \text{Im}\Xi_8 \bar{q}\tau_i \gamma^\mu t_a q \bar{q}\tau_j \gamma_\mu \gamma_5 t_a q). \end{aligned} \quad (8)$$

The tree-level matching of Eq. (8) to Eq. (3) is, for most operators, trivial. The qEDMs and qCEDMs are

$$\bar{m} d_{0,3} = -\frac{3v}{4} \text{Im} [(\Gamma_B^u + \Gamma_W^u)_{11} \mp 2(\Gamma_B^d - \Gamma_W^d)_{11}], \quad \bar{m} \tilde{d}_{0,3} = \frac{v}{2} \text{Im} (\tilde{\Gamma}^u \pm \tilde{\Gamma}^d)_{11}, \quad (9)$$

where the indices refer to generations. In most models $(\Gamma_{B,W}^{u,d})_{11}$ and $(\tilde{\Gamma})_{11}$ are proportional to the light-quark Yukawa couplings, thus canceling the light-quark mass on the left-hand-side of Eq. (9). The gCEDM gets tree-level contributions only from itself, and similarly for PS4QOs. The imaginary part of the right-handed current in Eq. (3) contributes to the $SU(2)_L$ -breaking LR4QOs. Thus, at tree level,

$$\text{Im}\Sigma_{1,8} = (\text{Im}\Sigma_{1,8})_{1111}, \quad \text{Im}\Xi_1 = V_{ud} (\text{Im}\Xi_1)_{11}, \quad \text{Im}\Xi_8 = 0, \quad (10)$$

where $V_{ud} \simeq 0.97$ is the up-down CKM element. $\text{Im}\Xi_8$ is, however, generated by the QCD evolution, as we discuss next. Note that all interactions in Eq. (8) are also \cancel{P} ; $P\cancel{\mathcal{X}}$ interactions are effectively of higher order and expected to produce even smaller effects.

2.2 Sizes and Runnings of \mathcal{X} Couplings

As the scale μ of interest decreases, one has to evolve the \mathcal{CP} coefficients. The $\bar{\theta}$ term is not multiplicatively renormalized because $\bar{\theta}$ is periodic, although it can mix with the divergence of the axial current [51]. The operators in Eq. (3) run from just below M_T to M_{EW} and the operators in Eq. (8) run from just below M_{EW} to M_{QCD} . Much of the literature concerns specific BSM models, where particular operators are singled out. A model-independent analysis to one loop, focusing on flavor-conserving interactions of the first generation, was carried out in Ref. [37], and the more general situation is under study [52].

For $M_T \sim$ a few TeV, the dominant effects in the evolution of coefficients are due to the strong interaction, and can be written in terms of the numbers of colors N_c and flavors n_f , the Casimir $C_F = (N_c^2 - 1)/2N_c$, and the beta function for $g_s = \sqrt{4\pi\alpha_s}$, $\beta_0 = (11N_c - 2n_f)/3$. The EW running for some of the operators has also been considered in Ref. [37], where earlier references can be found. The collection $\vec{C} = (\vec{C}_1, \vec{C}_2, \vec{C}_3)^T$ of $d = 6$ operators obeys the RG equation with a matrix γ of anomalous dimensions,

$$\frac{d\vec{C}(\mu)}{d\ln\mu} = \gamma\vec{C}(\mu), \quad \gamma = \frac{\alpha_s}{4\pi} \begin{pmatrix} \gamma_{\text{dip}} & \gamma_{\text{mix}} & \gamma_{13} \\ 0 & \gamma_{\text{PS}} & 0 \\ 0 & 0 & \gamma_{33} \end{pmatrix}. \quad (11)$$

Here $\vec{C}_1 = (d_0, d_3, \tilde{d}_0, \tilde{d}_3, d_W)^T$ and $\vec{C}_2 = (\text{Im}\Sigma_1, \text{Im}\Sigma_8)^T$. The renormalization and mixing of qEDMs, qCEDMs and gCEDM is described by [37, 53]

$$\gamma_{\text{dip}} = \begin{pmatrix} 8C_F & 0 & -8C_F & 0 & 0 \\ 0 & 8C_F & 0 & -8C_F & 0 \\ 0 & 0 & 16C_F - 4N_c & 0 & 2N_c \\ 0 & 0 & 0 & 16C_F - 4N_c & -2\varepsilon N_c \\ 0 & 0 & 0 & 0 & \beta_0 + N_c + 2n_f \end{pmatrix}, \quad (12)$$

while

$$\gamma_{\text{PS}} = 2 \begin{pmatrix} \beta_0 - 2(3 + 4/N_c)C_F & -2(1 + 1/N_c)^2(N_c - 2)C_F \\ 4(1 + 2/N_c) & \beta_0 + 2(C_F - 1 - 2/N_c^2) \end{pmatrix}, \quad (13)$$

$$\gamma_{\text{mix}} = \frac{1}{2} \begin{pmatrix} -5 + 3\varepsilon & 3 - 5\varepsilon & -4 & -4\varepsilon & 0 \\ (-5 + 3\varepsilon)C_F & (3 - 5\varepsilon)C_F & 2(N_c - 2C_F) & 2\varepsilon(N_c - 2C_F) & 0 \end{pmatrix}^T, \quad (14)$$

contain, respectively, the anomalous dimensions of singlet and octet PS4QOs [37, 54, 55], and the mixings of dipoles with PS4QOs [37, 55]. The first four columns of γ_{dip} are known to two loops [56].

Above M_{EW} , $\vec{C}_3 = (g_s^2 \text{Im}\Xi_1, \theta', \text{Im}Y'^u, \text{Im}Y'^d)^T$. The dipoles mix only with the gluon-Higgs operator θ' , whose diagonal entry vanishes [37, 57], the right-handed current operator $\text{Im}\Xi_1$ does not require renormalization [37], and the quark-Higgs couplings $\text{Im}Y'^{u,d}$ renormalize multiplicatively as the quark masses [37], so that

$$\gamma_{13} = -\frac{1}{2\pi^2 v^2} \begin{pmatrix} \vec{0} & (0 & 0 & 1 & \varepsilon & 0)^T & \vec{0} & \vec{0} \end{pmatrix}, \quad \gamma_{33} = -6C_F \begin{pmatrix} 0 & 0 & 0 & 0 \\ 0 & 0 & 1 & 0 \\ 0 & 0 & 0 & 1 \end{pmatrix}. \quad (15)$$

In these expressions we assumed that the qCEDM is proportional to the quark mass, and neglected terms with higher powers of quark masses.

Below M_{EW} , the quark-Higgs and gluon-Higgs operators disappear from the operator basis, and two new operators, the LR4QOs, appear: now $\vec{C}_3 = (\text{Im}\Xi_1, \text{Im}\Xi_8)^T$. These operators do not mix with the remaining operators and we have [37, 54, 55]

$$\gamma_{13} = \begin{pmatrix} \vec{0} & \vec{0} \end{pmatrix}, \quad \gamma_{33} = 2 \begin{pmatrix} \beta_0 & -3C_F/N_c \\ -6 & \beta_0 - 3N_c(1 - 2/N_c^2) \end{pmatrix}. \quad (16)$$

Besides the tree-level matching to coefficients of the Lagrangian (8), other tree-level contributions exist. For example, the quark-Higgs operator contributes to chiral-symmetry-breaking four-quark operators. However, these contributions are suppressed by additional powers of the EW scale, and are effectively of higher dimension—we refer to Ref. [37] for a discussion. Most loop corrections involve powers of α_{em} , which for simplicity we ignore. The gCEDM receives threshold corrections from the top CEDM, and, at lower energy, from the bottom and charm CEDMs [53]. At one loop, these contributions are finite, and, with our conventions, amount to a shift

$$\delta d_W(m_Q) = -\frac{\alpha_s(m_Q)}{8\pi} \tilde{d}_Q(m_Q) \quad (Q = t, c, b). \quad (17)$$

In the absence of the PQ mechanism, heavy quark CEDMs are also constrained by the large radiative corrections they induce in $\bar{\theta}$ [58]. When the Higgs is integrated out, $\bar{\theta}'$ generates an $\mathcal{O}(\alpha_s)$ threshold correction to the qCEDM, whose effect is however smaller than the qCEDM induced by running. Other important threshold corrections involve the top Yukawa coupling, and arise at two loops, through Barr-Zee type diagrams [59].

The overall effect of the RG is to modify the coefficients by factors which are typically of $\mathcal{O}(1)$ (except for $\text{Im}\Sigma_1$ which can get enhanced by almost an order of magnitude [37]). In Fig. 1 we illustrate effects of RG evolution. We consider cases where at the scale M_T only the gCEDM (continuous lines) or the top CEDM (dashed lines) exists. For the sake of illustration, we took $\tilde{d}_t(M_T) = -100 d_W(M_T)$. In the first case, we see that RG evolution reduces d_W to about 20% of its original value, while generating a qCEDM and, to a lesser extent, a qEDM. While we plotted only the isoscalar components, also the isovector qCEDM and qEDM are generated, in the proportion $\tilde{d}_3/\tilde{d}_0 = d_3/d_0 = \varepsilon \sim 1/3$. The tCEDM contributes to the gCEDM at the top threshold, Eq. (17), and generates light-quark qEDM and qCEDM through RG evolution. Although the induced gCEDM is a factor of 1000 smaller than \tilde{d}_t , the constraint from the neutron EDM is still about two orders of magnitude stronger than the direct bound from $t\bar{t}$ production at the LHC [60].

The main outcome of this analysis is that at $\mu \sim M_{\text{QCD}}$ the best organizational principle is given not by canonical dimension, but by the effective dimension inherited from the SM Lagrangian, Eq. (3). Thus all the coefficients in Eq. (8), including the q(C)EDMs, have sizes consistent with effective dimension six [35]:

$$d_i = \mathcal{O}\left(\frac{\delta_i}{M_T^2}\right), \quad \tilde{d}_i = \mathcal{O}\left(\frac{\tilde{\delta}_i}{M_T^2}\right), \quad d_W = \mathcal{O}\left(\frac{w}{M_T^2}\right), \quad \text{Im}\Sigma_a = \mathcal{O}\left(\frac{\sigma_a}{M_T^2}\right), \quad \text{Im}\Xi_a = \mathcal{O}\left(\frac{\xi}{M_T^2}\right), \quad (18)$$

where $\delta_{0,3}$, $\tilde{\delta}_{0,3}$, w , $\sigma_{1,8}$, and ξ are eight real parameters encoding details of the BSM physics. Naive dimensional analysis (NDA) [61, 62] suggests that these parameters are $\mathcal{O}(1)$. In contrast, six other \mathcal{CP} four-quark operators which are invariant under $SU(3) \times U(1)_{\text{em}}$ [54, 55] originate from either higher-dimensional operators at M_{EW} or higher-order electroweak effects, and are suppressed with respect to the PS4QOs and LR4QOs kept in Eq. (8) [35, 37].

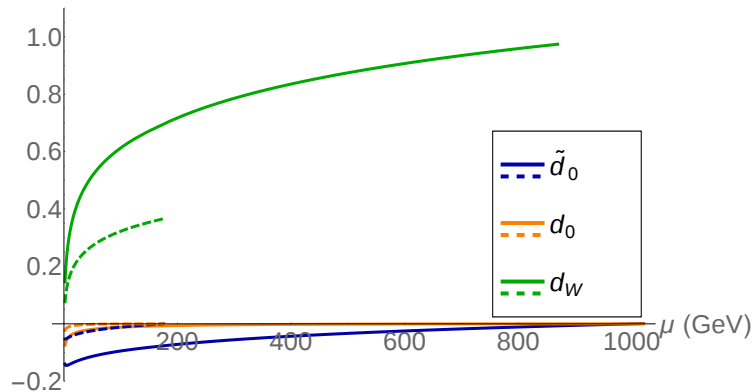


Figure 1: Examples of the RG evolution of $d = 6$ \mathcal{CP} operators: qCEDM \tilde{d}_0 , qEDM d_0 , and gCEDM d_W (in units of M_T^{-2}) as functions of the scale μ (in GeV). The only nonvanishing operator at $M_T \sim 1$ TeV is taken to be the gCEDM (continuous lines) or the top CEDM (dashed lines). For visibility, the qCEDM, qEDM and gCEDM originating in the tCEDM are multiplied by 100.

3 \mathcal{I} at the Hadronic Level

The \mathcal{I} interactions among quarks and gluons discussed in Section 2 translate, at low energies, into \mathcal{I} interactions involving the lightest mesons and baryons, which we sketch in this section.

3.1 Chiral Symmetry and Low-Energy Interactions

At a momentum comparable to the pion mass, $Q \sim m_\pi \ll M_{\text{QCD}}$, the implications of the Lagrangian in Eqs. (6) and (8) for the interactions among pions and nucleons are described by Chiral Perturbation Theory (χ PT) [63–65] and its extension to arbitrary number of nucleons, Chiral EFT [66–68]. The special role of the pion is a consequence of the invariance of Eq. (4) (for $e = 0$) under the chiral symmetry $SU(2)_L \times SU(2)_R \sim SO(4)$, and its spontaneous breaking to the isospin subgroup $SU(2)_V \sim SO(3)$. Pions emerge as Goldstone bosons whose interactions are proportional to their momenta, which guarantees that low-momentum observables can be computed in a perturbative expansion in powers of Q/M_{QCD} . Quark masses and other interactions explicitly break chiral symmetry, give pions masses, and induce non-derivative pion couplings, but the breaking is small and can be incorporated in the expansion. The chiral Lagrangian contains an infinite number of operators which can be grouped using a “chiral index” $\Delta = d + f/2 - 2 \geq 0$ that increases with the number d of derivatives and chiral-symmetry breaking parameters, and the number f of fermions. Assuming NDA, the prediction of any observable at a given accuracy in Q/M_{QCD} requires the consideration of only a finite number of operators, up to a certain Δ .

Chiral symmetry is realized nonlinearly in the chiral Lagrangian [69–71], whose construction via chiral-covariant objects is well known [72]. The choice of fields is arbitrary, and

for definiteness we employ a stereographic parametrization of the isospin-triplet $\boldsymbol{\pi}$, and an isospinor $N = (pn)^T$ for the nucleon. In this case the chiral-covariant derivatives take the form $D_\mu \pi_i = D^{-1}(\partial_\mu \delta_{ij} + eA_\mu \epsilon_{3ij})\pi_j$ and $\mathcal{D}_\mu N = [\partial_\mu + i\boldsymbol{\tau} \cdot \boldsymbol{\pi} \times D_\mu \boldsymbol{\pi}/F_\pi^2 + ieA_\mu(1 + \tau_3)/2]N$, with $F_\pi \simeq 186$ MeV the pion decay constant¹ and $D = 1 + \boldsymbol{\pi}^2/F_\pi^2$. Isospin-invariant objects are automatically chiral invariant; chiral-variant interactions are built with the $SO(4)$ transformation properties of the corresponding quark-gluon interactions. For example, electromagnetic interactions in Eq. (4) break chiral symmetry as an antisymmetric $SO(4)$ tensor [73]. Because $m_N \sim M_{\text{QCD}}$, Chiral EFT is well defined only for non-relativistic nucleons. The Q/m_N expansion can be made consistent with the Q/M_{QCD} expansion with heavy nucleon fields [74], when the nucleon mass m_N is removed from propagators and the Dirac structure simplifies to the nucleon velocity v^μ and spin S^μ . Resummations of the Q/m_N expansion are currently popular but they do not decrease the overall theoretical error. Chiral EFT can be extended to the Delta-isobar region using explicit fields for the Delta [75, 76] and the Roper [77], but most \mathcal{X} applications have so far been limited to nucleons. Chiral EFT reproduces the (B)SM S matrix because it includes all operators consistent with RG invariance and the symmetries of quark/gluon interactions at $\mu \sim M_{\text{QCD}}$.

Equation (4) is represented at lowest chiral index as

$$\begin{aligned} \mathcal{L}_T^{(0)} = & -\frac{1}{4}F_{\mu\nu}F^{\mu\nu} + \frac{1}{2}D_\mu \boldsymbol{\pi} \cdot D^\mu \boldsymbol{\pi} + \bar{N} \left(iv \cdot \mathcal{D} - \frac{2g_A}{F_\pi} S^\mu \boldsymbol{\tau} \cdot D_\mu \boldsymbol{\pi} \right) N \\ & + C_S \bar{N} N \bar{N} N + C_V \bar{N} \boldsymbol{\tau} N \cdot \bar{N} \boldsymbol{\tau} N, \end{aligned} \quad (19)$$

where $g_A = \mathcal{O}(1) \simeq 1.27$ is the pion-nucleon axial coupling and $C_{S,V}$ are LECs related to the two nucleon-nucleon scattering lengths. Higher-index interactions are constructed with further derivatives and nucleon fields. We assign a chiral index 3 to $\alpha_{\text{em}}/4\pi$, powers of which purely hadronic operators generated by the integration of hard photons —*e.g.*, the electromagnetic pion mass splitting $\delta m_\pi^2 = \mathcal{O}(\alpha_{\text{em}} M_{\text{QCD}}/4\pi) \simeq 1260$ MeV² [7]— are proportional to.

The properties under chiral symmetry of the operators in Eqs. (6) and (8) dictate how to incorporate them in the chiral Lagrangian, and determine the relative importance of \mathcal{X} couplings [33–35]. The average quark-mass term in Eq. (6) breaks chiral symmetry as the fourth component of an $SO(4)$ vector, and induces interactions proportional to powers of $\bar{m}r(\bar{\theta})$. The quark-mass splitting and the $\bar{\theta}$ term transform as different components of a single other $SO(4)$ vector, which implies that their hadronic matrix elements are directly related [32, 33]. They generate interactions proportional to powers of $\bar{m}\varepsilon r^{-1}(\bar{\theta})$ and $\bar{m}r^{-1}(\bar{\theta})(1 - \varepsilon^2) \sin \bar{\theta}/2$, respectively. For momenta $Q \sim m_\pi$, and taking $\varepsilon r^{-2}(\bar{\theta}) = \mathcal{O}(1)$, quark-mass terms are paired with chiral-symmetric operators by making d count powers of the pion mass as well. The lowest terms stemming from Eq. (6) are

$$\mathcal{L}^{(0,1)} = -\frac{m_\pi^2}{2D} \boldsymbol{\pi}^2 + \Delta m_N \left(1 - \frac{2\boldsymbol{\pi}^2}{F_\pi^2 D} \right) \bar{N} N + \frac{\delta m_N}{2} \bar{N} \left[\tau_3 - \frac{2\boldsymbol{\tau} \cdot \boldsymbol{\pi}}{F_\pi D} \left(\frac{\pi_3}{F_\pi} + \frac{1 - \varepsilon^2}{2\varepsilon} \sin \bar{\theta} \right) \right] N. \quad (20)$$

The pion mass is $m_\pi^2 = \mathcal{O}(M_{\text{QCD}} \bar{m}r(\bar{\theta}))$, the nucleon sigma term is $\Delta m_N = \mathcal{O}(m_\pi^2/M_{\text{QCD}})$, the neutron-proton mass splitting from the quark-mass difference is $\delta m_N = \mathcal{O}(\varepsilon r^{-2}(\bar{\theta}) m_\pi^2/M_{\text{QCD}})$,

¹ Note that the pion decay constant is frequently defined in the literature as $f_\pi = F_\pi/2$ or $f_\pi = F_\pi/\sqrt{2}$.

and pion-nucleon interactions — PT charge-symmetry breaking (CSB) for an even number of pions, \cancel{PT} for an odd number— are determined by the matrix element that enters δm_N . Similar relations exist at higher orders [33] —for example, involving the hadronic contribution to the pion mass splitting $\delta m_\pi^2 = \mathcal{O}(\delta m_N^2)$ — but the link between PT CSB and $\bar{\theta}$ operators quickly becomes superfluous.

The $d = 6$ operators in Eq. (8) have different transformation properties under chiral symmetry, and the connections with PT operators are more tenuous. The qCEDM and qEDM break chiral symmetry as $SO(4)$ vectors and induce both isospin-conserving and isospin-breaking \cancel{PT} interactions, which are in general of the same size because after aligning the $\bar{\theta}$ term there is no longer freedom to eliminate the qCEDM and qEDM isovector components. The important difference between qCEDM and qEDM is the suppression for the latter of purely hadronic operators by powers of $\alpha_{\text{em}}/4\pi$. The LR4QOs also break chiral symmetry (and isospin in particular), but as $SO(4)$ tensors, and the relative importance of their interactions is similar, but not identical, to the isovector qCEDM. The gCEDM and PS4QOs do not break chiral symmetry and cannot be distinguished purely on the basis of their symmetry properties, more information about their matrix elements being required. For chiral-invariant operators, chiral-breaking interactions, like non-derivative pion-nucleon couplings, are suppressed by factors of the quark masses.

The PT pion, pion-nucleon and multinucleon chiral Lagrangians are known up to $\Delta = 4, 3, 3$, respectively [78–81]. The Lagrangian from $\bar{\theta}$ and $d = 6$ operators was built in great detail in Refs. [33–36, 82–86]. For nucleon and light-nuclear EDMs at LO it is sufficient to consider a subset of the interactions discussed in Refs. [33–35]:

$$\begin{aligned} \mathcal{L}_T = & -\frac{1}{F_\pi} \bar{N} (\bar{g}_0 \boldsymbol{\tau} \cdot \boldsymbol{\pi} + \bar{g}_1 \pi_3) N - 2\bar{N} (\bar{d}_0 + \bar{d}_1 \tau_3) S^\mu N v^\nu F_{\mu\nu} \\ & - \frac{\bar{\Delta}}{F_\pi} \pi_3 \boldsymbol{\pi}^2 + \bar{C}_1 \bar{N} N \partial_\mu (\bar{N} S^\mu N) + \bar{C}_2 \bar{N} \boldsymbol{\tau} N \cdot \partial_\mu (\bar{N} S^\mu \boldsymbol{\tau} N). \end{aligned} \quad (21)$$

The operators that couple a neutral pion to the vacuum (pion tadpoles) can be eliminated order by order in favor of the interactions remaining in Eq. (21). Each of the operators in this equation has chiral partners, which we do not display explicitly. The interactions in the second line are only needed at LO for LR4QOs, PS4QOs, and gCEDM, while for qEDM only EDM-type operators in the first line are important. The coupling constants $\bar{g}_{0,1}$, $\bar{d}_{0,1}$, $\bar{C}_{1,2}$, and $\bar{\Delta}$ are discussed in the next section.

3.2 Sizes of \cancel{T} Couplings

The LECs in the \cancel{T} hadronic Lagrangian, Eq. (21), are (approximately) linear functions of $\bar{\theta}$ and of the coefficients of $d = 6$ operators in Eq. (8). We impose the constraints of chiral symmetry and use NDA for an estimate of the scaling of the LECs. In order to connect high-energy observables to EDMs, it is crucial that the coefficients of proportionality be known accurately. Going beyond NDA requires nonperturbative techniques, and we review here information that can be extracted using symmetry, LQCD simulations, and QCD sum rules. (A more comprehensive review of calculations of these matrix elements can be found in, for example, Ref. [43].)

The LECs \bar{g}_0 and \bar{g}_1 are isoscalar and isovector \mathcal{X} pion-nucleon couplings, which induce important long-range contributions to the nucleon EDM (Section 5) and to the \mathcal{X} nucleon-nucleon potential (Section 6.1). One expects [33, 35]

$$\bar{g}_0 = \mathcal{O} \left(\left(\frac{m_\pi^2}{M_{\text{QCD}}^2} \bar{\theta}, m_\pi^2 \tilde{d}_0, \varepsilon m_\pi^2 \tilde{d}_3, m_\pi^2 d_W, m_\pi^2 \text{Im} \Sigma_a, \varepsilon M_{\text{QCD}}^2 \text{Im} \Xi_a \right) M_{\text{QCD}} \right), \quad (22)$$

$$\bar{g}_1 = \mathcal{O} \left(\left(\frac{\varepsilon m_\pi^4}{M_{\text{QCD}}^4} \bar{\theta}, \frac{\varepsilon m_\pi^4}{M_{\text{QCD}}^2} \tilde{d}_0, m_\pi^2 \tilde{d}_3, \varepsilon m_\pi^2 d_W, \varepsilon m_\pi^2 \text{Im} \Sigma_a, M_{\text{QCD}}^2 \text{Im} \Xi_a \right) M_{\text{QCD}} \right). \quad (23)$$

Because $\bar{g}_{0,1}$ are LECs of chiral-breaking interactions, for most sources the quark masses appear. The contribution of isoscalar operators to \bar{g}_1 is suppressed by factors of m_π^2/M_{QCD}^2 , but as we discuss below \bar{g}_1 can still be important in systems, like the deuteron, for which the contribution of \bar{g}_0 vanishes. Isovector operators generate both \bar{g}_0 and \bar{g}_1 at the same order, even though \bar{g}_0 is affected by the quark mass difference. For all the operators in Eq. (8), a third non-derivative pion-nucleon coupling, $(\bar{g}_2/F_\pi) \bar{N} \pi_3 \tau_3 N$, is suppressed, and contributes at the same level as derivative \mathcal{X} couplings [33, 35], which we neglect.

Important consequences of chiral symmetry and vacuum alignment are the survival of the three-pion interaction $\bar{\Delta}$ and modifications of $\bar{g}_{0,1}$ proportional to it. Both $\bar{g}_{0,1}$ receive tree-level contributions. Moreover, at one loop $\bar{\Delta}$ gives a significant contribution to the pion-nucleon FF. Although formally an NLO effect, the loop is enhanced over NDA by a factor of 5π [35]. It endows the FF with a certain momentum dependence, whose effects on nucleon EDMs have not been studied. For light nuclei, they were found to be small [87]. We can capture the momentum-independent effects by redefining \bar{g}_1 . Thus,

$$\bar{g}_0 = g_0 + \frac{\delta m_N}{m_\pi^2} \bar{\Delta} + \dots, \quad \bar{g}_1 = g_1 + 2 \left(\frac{\Delta m_N}{m_\pi^2} - \frac{15 g_A^2 m_\pi}{16 \pi F_\pi^2} \right) \bar{\Delta} + \dots, \quad (24)$$

where $g_{0,1}$ are the couplings before alignment. The main remaining, explicit $\bar{\Delta}$ contribution is a tree-level three-nucleon potential (Section 6.1). Only for LR4QOs is $\bar{\Delta}$ an LO effect, while g_0 is higher order. In this case, we can eliminate [35],

$$\bar{\Delta} = \frac{m_\pi^2}{\delta m_N} \bar{g}_0 = \mathcal{O} (\text{Im} \Xi_a M_{\text{QCD}}^4). \quad (25)$$

The pion-nucleon couplings have been best studied when links to PT quantities through chiral symmetry are useful:

- For $\bar{\theta}$, a comparison between Eqs. (20) and (21), and similarly for higher-order terms, yields [32, 33],

$$\frac{\bar{g}_0}{F_\pi} = \frac{\delta m_N}{F_\pi} \frac{1 - \varepsilon^2}{2\varepsilon} \sin \bar{\theta} = (15 \pm 2) \cdot 10^{-3} \sin \bar{\theta}, \quad (26)$$

$$\frac{\bar{g}_1}{F_\pi} - \frac{g_1}{F_\pi} = \left(\frac{\Delta m_N}{m_\pi^2} - \frac{15 g_A^2 m_\pi}{16 \pi F_\pi^2} \right) \frac{\delta m_\pi^2}{F_\pi} \frac{1 - \varepsilon^2}{\varepsilon} \sin \bar{\theta} = -(4 \pm 3) \cdot 10^{-3} \sin \bar{\theta}, \quad (27)$$

using the values from LQCD, $\varepsilon = 0.37 \pm 0.03$ [88], $\delta m_N = 2.39 \pm 0.21$ MeV [89, 90], and $\Delta m_N = -63 \pm 9$ MeV [91], and from χ PT fitted to meson data, $\delta m_\pi^2 = 87 \pm 55$ MeV² [92]. This value for \bar{g}_0 is somewhat smaller than the NDA estimate. The relation between \bar{g}_0 and δm_N is violated by terms of $\mathcal{O}(m_\pi^2/M_{\text{QCD}}^2)$, an effect of the same size as the uncertainty in Eq. (26). g_1 is related to PT operators that contribute not to baryon masses, but to pion-nucleon scattering observables —however, only at an order beyond the current most precise analysis [93].

- For qCEDM, analogously [35, 94],

$$\bar{g}_0 = \delta m_N \left(\frac{\tilde{\delta} m_N \tilde{d}_0}{\delta m_N \tilde{c}_3} - \frac{\tilde{\Delta} m_\pi^2 \tilde{d}_3}{m_\pi^2 \tilde{c}_0} \right), \quad \bar{g}_1 = 2 \Delta m_N \left(\frac{\tilde{\Delta} m_N}{\Delta m_N} - \frac{\tilde{\Delta} m_\pi^2}{m_\pi^2} \right) \frac{\tilde{d}_3}{\tilde{c}_0}, \quad (28)$$

where $\tilde{c}_{0,3}$ are the coefficients of chromomagnetic operators analogous to the chromoelectric operators in Eq. (8), $\tilde{\Delta} m_\pi^2$, $\tilde{\Delta} m_N$, and $\tilde{\delta} m_N$ are corrections to the pion mass, nucleon sigma term, and nucleon mass splitting due to \tilde{c}_0 , \tilde{c}_0 , and \tilde{c}_3 , respectively. The evaluation of the corresponding matrix elements is currently being pursued by lattice collaborations [95]. At the moment, the best estimates on $\bar{g}_{0,1}$ come from QCD sum rules. It is found [11] that \bar{g}_1 is larger than \bar{g}_0 by a factor of about 5, and

$$\frac{\bar{g}_1}{F_\pi} = -(20_{-11}^{+40}) \cdot 10^{-3} (2\pi F_\pi)^2 \tilde{d}_3. \quad (29)$$

The large error is due to cancellations in Eq. (28), which complicate estimates of these couplings. In terms of dimensionless quantities, the numerical factors in Eqs. (26) and (29) are not very different, as one would expect from Eqs. (22) and (23).

The parameters $\bar{d}_{0,1}$ represent short-range contributions to the nucleon EDM (Section 5) and have expected sizes [33, 35]

$$\bar{d}_{0,1} = \mathcal{O} \left(\left(\frac{m_\pi^2}{M_{\text{QCD}}^2} \bar{\theta}, m_\pi^2 \tilde{d}_i, m_\pi^2 d_i, M_{\text{QCD}}^2 d_W, M_{\text{QCD}}^2 \text{Im} \Sigma_a, M_{\text{QCD}}^2 \text{Im} \Xi_a \right) \frac{e}{M_{\text{QCD}}} \right). \quad (30)$$

Chiral breaking intrinsic to the electromagnetic interaction ensures that no extra factors of quark masses are needed beyond those appearing explicitly in Eqs. (6) and (8). Because some of this breaking involves isospin, all sources induce isoscalar and isovector components of the same size. $\bar{d}_{0,1}$ are not fixed by symmetry but can be extracted from LQCD calculations of the nucleon EDMs, as we discuss in Sect. 5.2.

The remaining couplings in Eq. (21), $\bar{C}_{1,2}$, are less well known, and have not been studied extensively. They represent short-distance contributions to the nucleon-nucleon potential and their main phenomenological impact is through light-nuclear EDMs (Section 6). They are chiral-invariant interactions that appear without m_π^2/M_{QCD}^2 suppression, and at LO, only for chiral-invariant operators [35],

$$\bar{C}_{1,2} = \mathcal{O} \left((d_W, \text{Im} \Sigma_a) \frac{M_{\text{QCD}}}{F_\pi} \right). \quad (31)$$

For this reason, contact terms with different isospin structures are not needed at LO.

Equations (22)–(31) show how the different properties of $\bar{\theta}$ and $d = 6$ operators under chiral symmetry lead to different hierarchies among the couplings in Eq. (21), which has profound consequences for the EDM of the nucleon and light nuclei. Taking into account Eq. (25), these observables are expected to be described in LO in terms of the six independent LECs $\bar{g}_{0,1}$, $\bar{d}_{0,1}$, and $\bar{C}_{1,2}$. In Section 5 we find that the nucleon EDM depends mostly on $\bar{g}_{0,1}$ and $\bar{d}_{0,1}$, whereas in Section 6 we show that the six LECs enter nuclear EDMs. By contrast, the traditional description of nuclear \mathcal{X} is largely based on the three non-derivative pion couplings [96], $\bar{g}_{0,1}$ and \bar{g}_2 , which is subleading for all $d = 6$ sources.

4 Peccei-Quinn Mechanism

So far, we have assumed that there is no particular reason behind the small value of $\bar{\theta}$. A very elegant way to obtain a small $\bar{\theta}$ dynamically is the PQ mechanism [17], which is discussed in EFT in Ref. [97]. The approximate, spontaneously broken $U(1)_{PQ}$ symmetry is realized nonlinearly, with SM fields invariant and the pseudo-Goldstone boson, the axion a [18, 19], changing by an additive constant, $a \rightarrow a + c$. The symmetry is explicitly broken by the anomalous coupling to $G\tilde{G}$, which can be eliminated, as we did in Section 2.1, in favor of a complex quark mass term—except that now the axial rotation depends on a .

After vacuum alignment, which in this context is equivalent to the diagonalization of the pion-axion mass term, the axion Lagrangian reads

$$\begin{aligned} \mathcal{L}_{ax} = & \frac{1}{2} \partial_\mu a \partial^\mu a + \frac{1}{2f_a} \bar{q} [C_0 + (C_1 + \varepsilon r^{-2}(\bar{\theta} + a/f_a)) \tau_3] \gamma_5 \gamma_\mu q \partial^\mu a \\ & - \bar{m} r (\bar{\theta} + a/f_a) \bar{q} q + \varepsilon \bar{m} r^{-1} (\bar{\theta} + a/f_a) \bar{q} \left[\tau_3 + \frac{(1 - \varepsilon^2)}{2\varepsilon} \sin(\bar{\theta} + a/f_a) i\gamma_5 \right] q + \dots \end{aligned} \quad (32)$$

where f_a is the axion decay constant and the two couplings $C_{0,1}$ are model dependent. When chiral symmetry is broken, the term proportional to $\bar{q}q$ generates the axion potential $V(\bar{\theta} + a/f_a)$, whose minimum (curvature) determines the axion vev $\langle a \rangle$ (mass). If $\bar{\theta}$ is the only source of \mathcal{CP} , the potential is minimized by $\bar{\theta} + \langle a \rangle / f_a = 0$. The presence (in the “...”) of higher-dimensional \mathcal{CP} operators that break chiral symmetry affects this potential; for example for the qCEDM,

$$V(x) = -\frac{m_\pi^2 F_\pi^2}{4} r(x) \left[1 - \frac{\tilde{\Delta} m_\pi^2}{2\tilde{c}_0 m_\pi^2} (\tilde{d}_0 + \varepsilon \tilde{d}_3) r^{-2}(x) \sin x \right]. \quad (33)$$

Minimization results in an induced angle

$$\bar{\theta}_{\text{ind}} = \bar{\theta} + \frac{\langle a \rangle}{f_a} = \frac{2}{1 - \varepsilon^2} \frac{\tilde{\Delta} m_\pi^2}{\tilde{c}_0 m_\pi^2} (\tilde{d}_0 + \varepsilon \tilde{d}_3) \quad (34)$$

of $\mathcal{O}(M_{\text{QCD}}^2/M_T^2)$, similar to other $d = 6$ operators. The consequence to low-energy dynamics is that the coupling \bar{g}_0 induced by the qCEDM receives another correction,

$$(\bar{g}_0)_{\text{PQ}} = \bar{g}_0 + \delta m_N \frac{1 - \varepsilon}{2\varepsilon} \bar{\theta}_{\text{ind}} = \frac{\delta m_N}{\varepsilon \tilde{c}_3} \left(\varepsilon + \frac{\tilde{c}_3}{\tilde{c}_0} \frac{\tilde{\Delta} m_\pi^2}{m_\pi^2} \right) \tilde{d}_0, \quad (35)$$

which cancels the contribution from \tilde{d}_3 . Similar relations can be worked out for LR4QOs, resulting in a vanishing \bar{g}_0 .

5 Nucleon Electric Dipole Moment

The study of the nucleon EDM in χ PT has a long history starting with Ref. [32], where the leading pion-loop contribution to the neutron EDM induced by $\bar{\theta}$ was computed. The calculation was later extended to the radius [98] and then full [99] electric dipole form factor (EDFF), and to NLO [100–102]. The nucleon EDFF generated by the $d = 6$ operators was computed to NLO in Refs. [35, 103]. In addition to the EDM, the momentum dependence of the EDFF is interesting. Due to Schiff’s theorem [104], the nucleon EDM does not contribute to the EDM of atoms in the nonrelativistic limit, and the first non-vanishing contribution is induced by the EDFF radius. Furthermore, the EDFF presented in Section 5.1 can be used to guide the extrapolation of LQCD results in both pion mass [105–107] and momentum, as described in Section 5.2. The role of strangeness is examined in Section 5.3.

5.1 Chiral EFT

χ PT allows for the calculation of low-energy observables in a controlled perturbative expansion in powers of Q/M_{QCD} , where each loop contributes Q^2/M_{QCD}^2 [63]. A review, including the PT electric charge and magnetic dipole FFs, can be found in Ref. [108]. The $\cancel{P}T$ toroidal dipole FF can be found in Refs. [109, 110]. The $\cancel{P}\cancel{X}$ component of the electromagnetic current can be written as [99, 103]

$$J_{\cancel{P}\cancel{X}}^\mu(q, K) = 2 (F_0(Q^2) + F_1(Q^2)\tau_3) \left[S^\mu v \cdot q - S \cdot q v^\mu + \frac{1}{m_N} (S^\mu q \cdot K - S \cdot q K^\mu) + \dots \right], \quad (36)$$

where $q = p - p'$ and $K = (p + p')/2$ in terms of the nucleon momentum in the initial (final) state p (p'), and $Q^2 = -q^2 > 0$. Here $F_0(Q^2)$ ($F_1(Q^2)$) is the isoscalar (isovector) EDFF of the nucleon,

$$F_i(Q^2) = d_i - S'_i Q^2 + H_i(Q^2), \quad (37)$$

where d_i is the EDM, S'_i the Schiff moment, and $H_i(Q^2)$ accounts for the remaining Q^2 dependence.

For all \cancel{X} sources, to NLO [32, 35, 100–103]

$$\frac{d_n + d_p}{2} = \bar{d}_0 + \frac{eg_A \bar{g}_0}{(2\pi F_\pi)^2} \pi \left[\frac{3m_\pi}{4m_N} \left(1 + \frac{\bar{g}_1}{3\bar{g}_0} \right) - \frac{\delta m_N}{m_\pi} \right], \quad (38)$$

$$\frac{d_p - d_n}{2} = \bar{d}_1 + \frac{eg_A \bar{g}_0}{(2\pi F_\pi)^2} \left[L - \ln \frac{m_\pi^2}{\mu^2} + \frac{5\pi}{4} \frac{m_\pi}{m_N} \left(1 + \frac{\bar{g}_1}{5\bar{g}_0} \right) - \frac{\hat{\delta} m_\pi^2}{m_\pi^2} \right], \quad (39)$$

where $L = 2/(4 - d) - \gamma_E + \log 4\pi$, with d the spacetime dimension and $\gamma_E = 0.557\dots$ the Euler constant. For illustration, the leading diagrams are shown in Fig. 2. The nucleon magnetic dipole moment (MDM) couples to the electric field in the $\Delta = 2$ Lagrangian, an

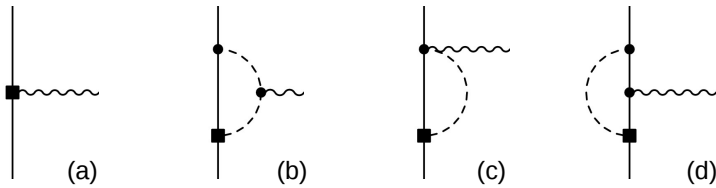


Figure 2: Leading diagrams for the nucleon EDM. Solid, dashed and wavy lines represent propagation of nucleons, pions and photons, respectively. Dots (squares) denote T (\mathcal{T}) interactions. For simplicity, only one possible ordering is shown.

effect $\propto m_N^{-2}$. It does not contribute to the EDM before next-to-next-to-leading order (N²LO), contrary to uncontrolled calculations based on a “relativistic” chiral Lagrangian [111]. The subset of $\mathcal{O}(1/m_N^2)$ corrections that are proportional to the MDM is small [112].

From the NDA estimates of Section 3.2, we see that the relative importance of the terms in Eqs. (38) and (39) depends on the source:

- $\bar{d}_{0,1}$, Fig. 2(a), dominates, while loop contributions, Fig. 2(b-d), appear at least at N²LO for qEDM, gCEDM, and PS4QOs. The full set of N²LO corrections was considered in Ref. [103].
- \bar{g}_0 appears at LO for sources that break chiral symmetry and do not contain photon fields: $\bar{\theta}$, qCEDM and LR4QOs. Its one-loop contribution is purely isovector, and the dependence on L and μ is eliminated solely by $\bar{d}_1(\mu)$. Non-analytic corrections to the isoscalar EDM are finite and suppressed by m_π/m_N . Despite the extra factor of π with respect to NDA, they are about 10% of the leading loop. However, one cannot exclude, on the basis of Eq. (30), that \bar{d}_0 is present at the same order. Without further dynamical information, one cannot state, as sometimes in the literature, that the nucleon EDM is isovector at this order.
- \bar{g}_1 contributes through recoil corrections in the nucleon propagator and pion-nucleon axial couplings, and only affects the proton EDM. In the case of isoscalar sources, \bar{g}_1 is formally suppressed by m_π^2/M_{QCD}^2 . Even for $\bar{\theta}$, where \bar{g}_0 is a factor of ten smaller than expected by power counting, \bar{g}_1 gives a correction to the proton EDM which is only a few percent of the leading loop. In the case of isospin-breaking sources, $\bar{g}_{0,1}$ appear at LO, but \bar{g}_0 arises from pion tadpoles and is proportional to δm_N , which makes it numerically smaller than \bar{g}_1 [35]. For the isovector qCEDM and LR4QO, then, the nucleon EDM is likely to receive its largest numerical contribution from the LECs $\bar{d}_{0,1}$, with non-analytic terms entering at the 30% level.

For concreteness, we specify Eqs. (38) and (39) for $\bar{\theta}$, where \bar{g}_0 is well determined by Eq. (26) and \bar{g}_1 gives only an N³LO effect. Setting the renormalization scale $\mu = m_N$ and

neglecting the numerically small isospin-breaking contributions,

$$d_n - (\bar{d}_0 - \bar{d}_1) = -\frac{eg_A\bar{g}_0}{(2\pi F_\pi)^2} \left[\ln \frac{m_N^2}{m_\pi^2} + \frac{\pi m_\pi}{2 m_N} \right] \bar{\theta} = -(1.99 + 0.12) \cdot 10^{-3} \sin \bar{\theta} \text{ e fm}, \quad (40)$$

$$d_p - (\bar{d}_0 + \bar{d}_1) = \frac{eg_A\bar{g}_0}{(2\pi F_\pi)^2} \left[\ln \frac{m_N^2}{m_\pi^2} + 2\pi \frac{m_\pi}{m_N} \right] \bar{\theta} = (1.99 + 0.46) \cdot 10^{-3} \sin \bar{\theta} \text{ e fm}, \quad (41)$$

showing that, especially for the neutron, convergence of the $SU(2)$ chiral expansion is good. Assuming that there are no fine-tuned cancellations [32] between $\bar{d}_{0,1}$, which are analytic in m_π^2 , and non-analytic contributions, the current bound on d_n [9] allows to put a bound on $\bar{\theta}$. Similarly, using the NDA expressions for $\bar{g}_{0,1}$ and $\bar{d}_{0,1}$ given in Section 3.2 and assuming no cancellations, one can bound the coefficients of $d = 6$ operators [103]:

$$\bar{\theta}, M_{\text{QCD}}^2 \bar{d}_i, M_{\text{QCD}}^2 d_i \lesssim 10^{-10}, \quad M_{\text{QCD}}^2 d_W, M_{\text{QCD}}^2 \text{Im}\Sigma_a, M_{\text{QCD}}^2 \text{Im}\Xi_a \lesssim 10^{-12}. \quad (42)$$

The weaker bound on $\bar{\theta}$, qCEDM and qEDM reflects the proportionality to light-quark masses. If the dimensionless \mathcal{X} parameters in Eq. (18) are $\mathcal{O}(1)$, the bounds in Eq. (42) suggest new physics at a scale $M_T \gtrsim 100$ TeV. Once NDA can be replaced by more accurate determinations of matrix elements in LQCD, these bounds can be reliably translated into bounds on the dimensionless parameters at M_T using the RG of Section 2.2, as sketched in Ref. [37].

While certainly an exciting evidence of new physics, the observation of neutron *and* proton EDMs would not, with the current theoretical status, be sufficient to clearly identify the source of new physics, and in particular to disentangle the effect of $\bar{\theta}$ from higher-dimension operators. Without further input from nonperturbative techniques, Eqs. (40) and (41) show that, for all operators in Eq. (8), $d_{p,n}$ contain at least two unknown LECs. An interesting independent observable is the momentum dependence of the EDFF. To NLO [35,98,99,102,103], the square radii are

$$S'_0 = -\frac{\pi eg_A\bar{g}_0\delta m_N}{12(2\pi F_\pi)^2 m_\pi^3}, \quad S'_1 = \frac{eg_A\bar{g}_0}{6(2\pi F_\pi)^2 m_\pi^2} \left(1 - \frac{5\pi m_\pi}{4 m_N} - \frac{\hat{\delta} m_\pi^2}{m_\pi^2} \right). \quad (43)$$

For $\bar{\theta}$, qCEDM and LR4QO, radii arise at the same order as the EDM, are finite in the chiral limit and approximately isovector. They are dominated by contributions at the scale m_π , which are known except for the \mathcal{X} parameters. For example, for $\bar{\theta}$ [102],

$$S'_0 = -5.0 \cdot 10^{-6} \sin \bar{\theta} \text{ e fm}^3, \quad S'_1 = 6.8 \cdot 10^{-5} \sin \bar{\theta} \text{ e fm}^3. \quad (44)$$

In contrast, for qEDM, gCEDM and PS4QOs, radii arise at N²LO and scale as Q^2/M_{QCD}^2 with respect to the EDM [103]. The functions $H_i(Q^2)$ from Eq. (37) can be found, to NLO, in Refs. [35,99,102,103]. Although an experimental measurement of the momentum dependence of the EDFF is not going to happen any time soon, the extrapolation $Q^2 \rightarrow 0$ of LQCD EDFFs for $\bar{\theta}$ and qCEDM would allow to extract \bar{g}_0 and $\bar{d}_{0,1}$ at the same time.

5.2 Interplay with Lattice QCD

The best tool to determine the LECs $\bar{d}_{0,1}$ that contribute to the nucleon EDM is LQCD. Unfortunately there are virtually no LQCD results for the $d = 6$ sources, most work having focused on $\bar{\theta}$. A collection of early results can be found in Ref. [113].

A recent LQCD evaluation of $d_{p,n}$ from $\bar{\theta}$ can be found in Ref. [114]. Simulations were performed at two values of the pion mass, $m_\pi = 330, 420$ MeV, with domain-wall fermions to suppress the lattice artifact of chiral symmetry violation. Results, which still have a significant statistical error, are extrapolated linearly to $Q = 0$, where they give EDMs compatible with zero. Ref. [107] improved the finite-volume corrections of Refs. [105,106] and used these LQCD results to extract $\bar{d}_{0,1}$ with $SU(3)$ χ PT at NLO. We have fitted the same EDM points but with the $SU(2)$ formulas, Eqs. (38) and (39), and neglecting finite-volume corrections. We find good fits, as exemplified for the isovector component in Fig. 3, where the best fit results and 1σ uncertainty obtained from Eq. (39), with \bar{g}_0 fixed to the value (26), are compared with results of fitting \bar{d}_1 only and neglecting the chiral loop, that is, setting \bar{g}_0 to zero. Clearly, lattice EDM data show an essentially linear dependence on m_π^2 with no clear sign of the chiral log. For the short-range LECs at the scale $\mu = 939$ MeV, we find, factoring out the pion-mass dependence,

$$\bar{d}_0(\mu) = (-0.04 \pm 0.45) \frac{m_\pi^2}{(2\pi F_\pi)^3} e \sin \bar{\theta}, \quad \bar{d}_1(\mu) = (0.05 \pm 0.45) \frac{m_\pi^2}{(2\pi F_\pi)^3} e \sin \bar{\theta}, \quad (45)$$

which is not far from the NDA estimate of Section 3.2, once one considers the large uncertainties. Extrapolating to the physical pion mass, again using Eq. (26),

$$d_n = -(2.4 \pm 1.5) \cdot 10^{-3} \sin \bar{\theta} e \text{ fm}, \quad d_p = (2.5 \pm 1.5) \cdot 10^{-3} \sin \bar{\theta} e \text{ fm}, \quad (46)$$

which are consistent with the more sophisticated analysis of Ref. [107]. After this review was completed, an LQCD calculation with clover fermions and imaginary $\bar{\theta}$ has appeared [115], which gives a similar value for d_n but with smaller error bars.

Eventually, the extrapolation in Q^2 could also be made with the full χ PT EDFF, Eq. (37) [35, 99, 102, 103]. The range in Q used in Ref. [114] (from about 450 to 800 MeV) is unfortunately beyond the validity of χ PT, but new calculations, already under way at a lighter pion mass ($m_\pi = 170$ MeV), are performed at smaller Q^2 [116]. They should make it possible to extract \bar{g}_0 by fitting the slope of the EDFF with the χ PT prediction in Eq. (43), and to check the estimate in Eq. (26).

The uncertainty on the LQCD evaluation of $\bar{d}_{0,1}$ is quite large and compatible with zero. Nonetheless, for $\bar{\theta}$ LQCD is now competitive with other nonperturbative techniques. For comparison, from QCD sum rules [117–119],

$$|d_n| = (2.5 \pm 1.3) \cdot 10^{-3} \bar{\theta} e \text{ fm}. \quad (47)$$

QCD sum rules also give the best available estimate for the qCEDM [120],

$$|d_n| = (1 \pm 0.5) (2\pi F_\pi)^2 |0.9 \tilde{d}_0 - 0.3 \tilde{d}_3| \cdot 10^{-3} e \text{ fm}. \quad (48)$$

Among $d = 6$ sources, the qEDM is particularly simple, since to a good approximation $d_{p,n}$ arise solely from $\bar{d}_{0,1}$ with small isospin-breaking corrections. From Eqs. (8) and (21), the photon couples in LO to the isoscalar and isovector tensor charges defined by $\langle N | \bar{q} \sigma_{\mu\nu} q | N \rangle = 4g_0^T \epsilon^{\mu\nu\rho\sigma} v_\rho \bar{N} S_\sigma N$, $\langle N | \bar{q} \sigma_{\mu\nu} \tau_3 q | N \rangle = 4g_1^T \epsilon^{\mu\nu\rho\sigma} v_\rho \bar{N} S_\sigma \tau_3 N$, resulting in

$$\frac{d_n + d_p}{2} = g_0^T \bar{m} e \left(\frac{d_0}{3} + d_3 \right) = (0.29 \pm 0.03) \bar{m} e \left(\frac{d_0}{3} + d_3 \right), \quad (49)$$

$$\frac{d_p - d_n}{2} = g_1^T \bar{m} e \left(d_0 + \frac{d_3}{3} \right) = (0.51 \pm 0.04) \bar{m} e \left(d_0 + \frac{d_3}{3} \right), \quad (50)$$

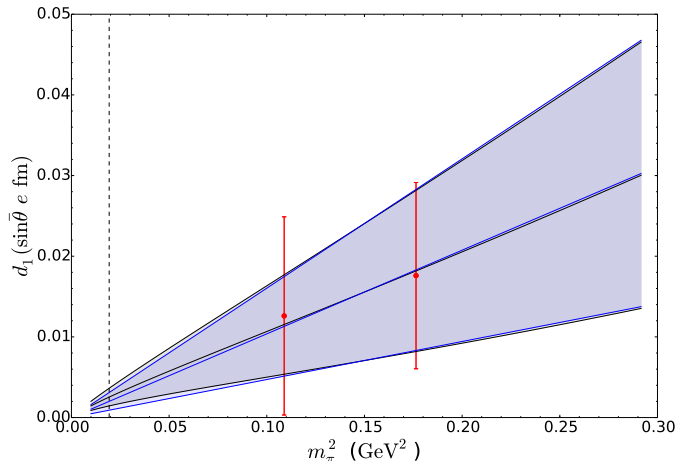


Figure 3: Isovector component d_1 of the nucleon EDM (in units of $\sin\bar{\theta} e \text{ fm}$) as function of the pion mass squared m_π^2 (in units of GeV^2). The black lines and gray shaded area show the best fit and 1σ uncertainty obtained by fitting Eq. (39) to the LQCD results of Ref. [114], represented by the red points with error bars. The blue lines and blue shaded area are the corresponding fit with $\bar{g}_0 = 0$. The dashed vertical line indicates the physical pion mass.

where we used the recent LQCD results [121–123] for the proton tensor charges at $\mu = 2 \text{ GeV}$, and quark mass and qEDM should also be evaluated at this scale. These numbers are in good agreement with the NDA expectation. Existing extractions of the proton tensor charges from experiment [124, 125] are at too high a Q^2 for χ PT. Some of the issues affecting the lattice implementation of higher-dimensional operators are discussed in Ref. [126].

Our simplified analysis of LQCD data, which omitted correlations, finite-volume effects and systematic errors, suggests that there can be a rich interplay between LQCD and χ EFT. It will be interesting to see whether the substantial reduction of the LQCD uncertainty to the 10% level expected in the near future for $\bar{\theta}$ [114] will show a clear signal of an EDM and the presence of a chiral logarithm, allowing an extraction of \bar{g}_0 . More generally, LQCD calculations of matrix elements for other sources would fill a gaping hole in the road from BSM physics to EDM experiments.

5.3 Role of Strangeness

Much of the low-energy \mathcal{N} literature includes the strange quark s explicitly. Yet, the intermediate value of its mass m_s poses a problem: it prevents integrating s out at a perturbative scale, as it is done for the t , b and, to a lesser extent, c quarks, but leads to poor convergence of the χ PT expansion via a relatively large kaon mass m_K [127]. Although the best way to deal with s (and maybe also c) is through nonperturbative techniques, symmetry considerations also give some insight.

$\bar{\theta}$ effects in $SU(3)_L \times SU(3)_R$ ($U(3)_L \times U(3)_R$) if one wants an explicit connection to the

$U(1)_A$ anomaly) χ PT [82–86] are proportional to

$$\frac{m_d m_u m_s}{m_s(m_d + m_u) + m_u m_d} = \frac{\bar{m}}{2}(1 - \varepsilon^2) \left[1 + \frac{\bar{m}}{m_s}(1 - \varepsilon^2) + \dots \right]. \quad (51)$$

Although \bar{g}_0 and δm_N receive, starting at order $\mathcal{O}(m_K/M_{\text{QCD}})$, large corrections from kaon and eta meson loops (which show little sign of convergence), these corrections affect \bar{g}_0 and δm_N in exactly the same way up to N²LO and are already accounted for through Eq. (26) when extracting δm_N from LQCD simulations with dynamical strange quarks. At N²LO, in both $SU(2)$ and $SU(3)$ χ PT there are short-distance contributions to \bar{g}_0 that do not affect δm_N , but, since they are not proportional to m_s , their numerical effect should not be larger than the uncertainty quoted in Eq. (26). The isospin-violating coupling \bar{g}_1 receives a tree-level contribution proportional to the π - η mixing angle, which, despite being formally LO, is suppressed with respect to \bar{g}_0 by \bar{m}/m_s and is numerically of the same size as the estimate of Eq. (27). The first contribution not suppressed by powers of \bar{m}/m_s appears at N²LO, as in $SU(2)$ χ PT. Thus, strangeness should not significantly affect the values of the pion-nucleon couplings from $\bar{\theta}$.

The nucleon EDM has been computed in this framework to various degrees of sophistication [32, 101, 106]. At one loop, there are additional nucleon-kaon and nucleon-eta couplings, which at LO are fixed by combinations of baryon masses, for example $\bar{g}_{N\Sigma K}$ is related to the mass difference between the nucleon and the Σ baryon, $m_N - m_\Sigma$. As for \bar{g}_0 , these relations are violated at N²LO. However, now the corrections are proportional to m_s , and are numerically more important [128]. For the nucleon, pion and kaon loops give contributions of approximately the same size. However, NLO corrections to the kaon contributions are as large as LO, casting some doubts on the convergence of the $SU(3)$ expansion. On the contrary, the $SU(2)$ expansion of the nucleon EDM converges fairly well.

In the $d = 6$ sector, the basis in Eq. (8) needs to be enlarged to include s . Four additional quark bilinears can be constructed, the strange EDM (sEDM) and CEDM (sCEDM), and two $\Delta S = 1$ flavor-changing neutral currents of the same form as the qEDM and qCEDM but containing a d and an s . There are also several more four-quark operators, listed in Ref. [54], which, however, does not fully account for the constraint of SM gauge symmetry. If one considers only $\Delta S = 0$ operators, in addition to the four operators already defined in Eq. (8), eight four-quark operators with two strange quark fields receive non-vanishing matching coefficients at tree level, so that only half of the operators defined Ref. [54] needs to be considered. The matrix elements of these operators were studied [54] in the factorization approximation and in the quark model, but more rigorous techniques are needed.

The sEDM and sCEDM have received more attention. The effect of the sEDM d_s on $d_{p,n}$ can be obtained from $\langle N | \bar{s} \sigma^{\mu\nu} s | N \rangle = 2g_s^T \epsilon^{\mu\nu\rho\sigma} v_\rho \bar{N} S_\sigma N$ on the lattice: factoring out the strange quark mass and charge, as in Eq. (8), $d_n + d_p = -2g_s^T m_s d_s / 3$. g_s^T involves sea quarks, and is numerically more challenging to calculate on the lattice than $g_{u,d}^T$. A recent, state-of-the-art LQCD calculation [121] finds $g_s^T = 0.002 \pm 0.011$. With these large uncertainties, it is not possible to exclude that, due to the enhancement $m_s/m_d \sim 20$, the sEDM gives a contribution to $d_n + d_p$ of the same size as Eq. (49). The contribution of the sCEDM \tilde{d}_s has been addressed in $SU(3)$ χ PT and QCD sum rules [11, 55, 129]. Refs. [55, 129] found that \tilde{d}_s could give a large, possibly dominant, contribution to the nucleon EDM. In the presence of

PQ symmetry, \tilde{d}_s does not contribute at LO to pion-nucleon \mathcal{Z} couplings, but affects $\bar{g}_{N\Sigma K}$ and thus induces long-range contributions. The numerical value of the loop is small, but not so small as to compensate the enhancement due to the appearance of m_s in the coefficient of the sCEDM. It would be interesting to test the robustness of this prediction by going beyond LO. In general, the same issue as for $\bar{\theta}$ remains: the convergence of $SU(3)$ χ PT.

6 \mathcal{Z} Moments of Light Nuclei

The observation of neutron and proton EDMs will not provide enough information to clearly identify the leading \mathcal{Z} source(s). \mathcal{Z} in light nuclei, being sensitive to different combinations of the couplings in Eq. (21), is highly complementary, and it can be computed in the same theoretical framework as the nucleon EDFFF with reliable accuracy. For these reasons, and with the additional motivation of the exciting experimental developments that might allow a direct measurement of EDMs of charged ions, the study of the EDMs of deuteron, helion and triton has received a lot of attention in the last few years, both from a phenomenological perspective [130–134] and with Chiral EFT [87, 135–137]. Very recently, the first model calculation of the ${}^6\text{Li}$ EDM has appeared [138]. For the deuteron, as seen in Tab. 1, two other moments, MQM and TQM, are sensitive to \mathcal{Z} and have been calculated for $d \leq 6$ \mathcal{Z} sources in Refs. [135, 139] and [140], respectively, but prospects for their detection are remote at best. \mathcal{Z} in neutron-proton [141] and neutron-deuteron [142] scattering have been revisited recently, but seem equally difficult to measure.

\mathcal{Z} is a small effect, and can be treated perturbatively on top of the strong nuclear interactions. The elements that enter EFT calculations in nuclei are discussed in Section 6.1, while results for nucleon number $A = 2, 3$ are reviewed in Section 6.2. The alpha particle ($A = 4$) has no \mathcal{Z} moments, but \mathcal{Z} FFs of nuclei with a few more nucleons could be calculated within this approach.

6.1 Nuclear Potential and Currents

The \mathcal{Z} electromagnetic current can be written in the form of Eq. (36) for a spin-1/2 nucleus, and in a straightforward generalization that includes MQM [135] and TQM [140] for spin-1. It receives several contributions, schematically illustrated in Fig. 4. The nuclear wavefunction, denoted by the shaded triangles, as well as the iteration of the PT potential V_{PT} , represented by the shaded blob, can be obtained by solving the Schrödinger equation. \mathcal{Z} , denoted by black squares, either affects the electromagnetic current (Fig. 4(a)) or perturbs the nuclear wavefunction with an insertion of the \mathcal{Z} potential (Fig. 4(b)).

The power counting of Chiral EFT systematically organizes the various contributions [35, 136]. While in the one-nucleon sector a loop brings in a suppression of Q^2/M_{QCD}^2 , in problems with two or more nucleons a relative enhancement of $4\pi m_N/Q$ compensates the loop suppression in diagrams that involve intermediate states with nonrelativistic nucleons only, where energies are $\mathcal{O}(Q^2/m_N)$ rather than $\mathcal{O}(Q)$ as in χ PT [30]. The one-body contribution in Fig. 4(a) represents the nuclear FF arising from the EDFFF of the constituents, Eq. (37). The PT one-nucleon current contribution to Fig. 4(b) contains an additional loop with

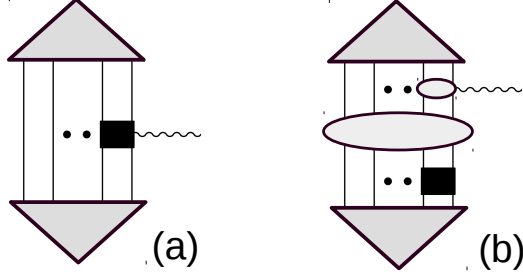


Figure 4: Contribution to nuclear EDMs. The large triangles denote the nuclear PT wavefunction; the oval, iterations of the PT potential; the oval with an attached photon, a few-nucleon current; the black square, the \mathcal{Z} potential; and the large black square with an attached photon, a \mathcal{Z} few-nucleon current. Other notation as in Fig. 2.

respect to the one-body contribution in Fig. 4(a). These contributions scale as

$$J_a = \mathcal{O}(F_{0,1}Q), \quad J_b = \mathcal{O}\left(\frac{e\bar{g}_{0,1}}{F_\pi^2}Q, e\bar{C}_{1,2}F_\pi^2Q, \frac{e\bar{\Delta}}{F_\pi^2M_{\text{QCD}}}Q\right). \quad (52)$$

Depending on the sizes of $\bar{g}_{0,1}$ compared to $d_{n,p}$, insertions of two-body currents in Fig. 4(b) can be as big as the one-body contribution to Fig. 4(a) [136].

The various ingredients in Fig. 4 can be obtained explicitly in terms of the \mathcal{Z} LECs. For EDMs, the most important \mathcal{Z} current is the sum of one-body contributions,

$$J_{T,1}^0(\vec{q}) = -\frac{i}{2} \sum_i \left[d_n + d_p + (d_p - d_n) \tau_3^{(i)} \right] \vec{\sigma}^{(i)} \cdot \vec{q}, \quad (53)$$

where $\vec{\sigma}^{(i)}/2$ ($\vec{\tau}^{(i)}/2$) is the spin (isospin) of the nucleon i that interacts with the photon, and \vec{q} is the (outgoing) photon momentum. Pion-exchange \mathcal{Z} currents induced by \bar{g}_0 , which by power counting could be important for the deuteron EDM from $\bar{\theta}$, are given in Ref. [136], but their contribution is found to be numerically small.

The tree-level potential induced by the couplings in Eq. (21) has a two-body component [34], which is generated by one-pion exchange (OPE) with couplings $\bar{g}_{0,1}$ and by the short-range interactions $\bar{C}_{1,2}$,

$$V_{T,2}(\vec{k}_i) = \frac{i}{2F_\pi^2} \sum_{j>i} \vec{k}_i \cdot \left\{ \left[-F_\pi^2 \bar{C}_1 + \left(\frac{2g_A \bar{g}_0}{\vec{k}_i^2 + m_\pi^2} - F_\pi^2 \bar{C}_2 \right) \vec{\tau}^{(i)} \cdot \vec{\tau}^{(j)} \right] (\vec{\sigma}^{(i)} - \vec{\sigma}^{(j)}) + \frac{g_A \bar{g}_1}{\vec{k}_i^2 + m_\pi^2} \left[(\tau_3^{(i)} + \tau_3^{(j)}) (\vec{\sigma}^{(i)} - \vec{\sigma}^{(j)}) + (\tau_3^{(i)} - \tau_3^{(j)}) (\vec{\sigma}^{(i)} + \vec{\sigma}^{(j)}) \right] \right\}, \quad (54)$$

and a three-body component [35], which is generated by the three-pion coupling $\bar{\Delta}$,

$$V_{T,3}(\vec{k}_i) = -\frac{2g_A^3 \bar{\Delta}}{F_\pi^4} \sum_{k>j>i} \left(\tau_3^{(i)} \vec{\tau}^{(j)} \cdot \vec{\tau}^{(k)} + \tau_3^{(j)} \vec{\tau}^{(i)} \cdot \vec{\tau}^{(k)} + \tau_3^{(k)} \vec{\tau}^{(i)} \cdot \vec{\tau}^{(j)} \right) \times \frac{\vec{\sigma}^{(i)} \cdot \vec{k}_i \vec{\sigma}^{(j)} \cdot \vec{k}_j \vec{\sigma}^{(k)} \cdot \vec{k}_k}{(\vec{k}_i^2 + m_\pi^2)(\vec{k}_j^2 + m_\pi^2)(\vec{k}_k^2 + m_\pi^2)}, \quad (55)$$

Source	$\bar{\theta}$	qCEDM	qEDM	gCEDM, PS4QOs	LR4QOs
$M_{\text{QCD}}d_n/e$	$\mathcal{O}\left(\frac{m_\pi^2}{M_{\text{QCD}}^2}\bar{\theta}\right)$	$\mathcal{O}\left(\frac{m_\pi^2}{M_T^2}\tilde{\delta}_i\right)$	$\mathcal{O}\left(\frac{m_\pi^2}{M_T^2}\delta_i\right)$	$\mathcal{O}\left(\frac{M_{\text{QCD}}^2}{M_T^2}(w, \sigma_a)\right)$	$\mathcal{O}\left(\frac{M_{\text{QCD}}^2}{M_T^2}\xi\right)$
d_p/d_n	$\mathcal{O}(1)$	$\mathcal{O}(1)$	$\mathcal{O}(1)$	$\mathcal{O}(1)$	$\mathcal{O}(1)$
d_d/d_n	$\mathcal{O}(1)$	$\mathcal{O}\left(\frac{M_{\text{QCD}}^2}{Q^2}\right)$	$\mathcal{O}(1)$	$\mathcal{O}(1)$	$\mathcal{O}\left(\frac{M_{\text{QCD}}^2}{Q^2}\right)$
d_h/d_n	$\mathcal{O}\left(\frac{M_{\text{QCD}}^2}{Q^2}\right)$	$\mathcal{O}\left(\frac{M_{\text{QCD}}^2}{Q^2}\right)$	$\mathcal{O}(1)$	$\mathcal{O}(1)$	$\mathcal{O}\left(\frac{M_{\text{QCD}}^2}{Q^2}\right)$
d_t/d_h	$\mathcal{O}(1)$	$\mathcal{O}(1)$	$\mathcal{O}(1)$	$\mathcal{O}(1)$	$\mathcal{O}(1)$

Table 2: Expected orders of magnitude for the neutron EDM (in units of e/M_{QCD}), and for the EDM ratios proton to neutron, deuteron to neutron, helion to neutron, and triton to helion, for $\bar{\theta}$ and $d = 6$ sources. Q represents the low-energy scales F_π , m_π , and $\sqrt{m_N B}$, with B the binding energy. (Adapted from Ref. [136].)

where \vec{k}_i is the momentum transferred from nucleon i . The OPE potential generated by the couplings $\bar{g}_{0,1}$ is well known [96]. It should be important for $\bar{\theta}$, qCEDM, gCEDM, PS4QOs, and LR4QOs, but for the $\bar{\theta}$ only \bar{g}_0 appears at LO. The short-range terms, which can be thought as the long-wavelength effect of \mathcal{X} heavy meson exchange, should be kept at this order for gCEDM and PS4QOs. The three-body force, which is new, appears at LO only for LR4QOs. The LO potential induced by the qEDM is given in Ref. [34], but it is of little phenomenological relevance. Chiral EFT provides a framework to go beyond LO by including two-pion exchange potentials, relativistic corrections, and OPE potentials from subleading couplings. For $\bar{\theta}$, N²LO corrections to Eq. (54) were discussed in Ref. [34]. The calculation can be immediately extended to the qCEDM, with the observation that TPE diagrams involving \bar{g}_1 vanish [137]. In the case of the LR4QO, the coupling $\bar{\Delta}$ gives a relatively large NLO correction to the isospin-breaking OPE potential [35, 87], the largest part of which we absorbed in \bar{g}_1 (Eq. (24)).

6.2 Moments

The estimate of Eq. (52), combined with the relative sizes of $\bar{g}_{0,1}$, $\bar{d}_{0,1}$, $\bar{C}_{1,2}$ and $\bar{\Delta}$ discussed in Section 3.2, lead to the expectation that for qCEDM and LR4QOs EDMs of light nuclei are dominated by the \mathcal{X} OPE potential. For the gCEDM and PS4QOs, one-body, OPE and $\bar{C}_{1,2}$ contributions should be approximately equal, while if the qEDM is the only \mathcal{X} source light-nuclear EDMs are well approximated by the EDMs of the constituents. For $\bar{\theta}$, the situation is more complicated. For most nuclei, OPE from \bar{g}_0 should dominate, but when the numbers of protons and neutrons are equal, $N = Z$, spin/isospin selection rules cause isoscalar \mathcal{X} interactions, such as \bar{g}_0 and $\bar{C}_{1,2}$, not to contribute [143] at LO. $N = Z$ nuclei like the deuteron are mainly sensitive to isovector couplings, in particular \bar{g}_1 , and the EDM from $\bar{\theta}$ is suppressed by Q^2/M_{QCD}^2 with respect to the naive expectation in Eq. (52). Using Eq. (18) we obtain the order-of-magnitude estimates for $d_{d,t,h}$ in Tab. 6.2, which indicates that light-nuclear EDM measurements would offer clues regarding \mathcal{X} sources. Expectations about the deuteron MQM are described in Ref. [139].

In principle, light-nuclear EDMs can be calculated consistently within EFT. Light nuclei are sufficiently diluted to be studied in an EFT where pions are integrated out [30], but in this case one cannot easily keep track of the chiral-symmetry constraints discussed in Section 3. For such nuclei, the pions present in Chiral EFT can be treated in perturbation theory [144], in which case only contact interactions need to be included in the PT sector at LO. For the deuteron, the PT [145] and \cancel{PT} [146] electromagnetic FFs have been calculated quite successfully in this framework. This framework was extended to $\cancel{\mathcal{J}}$ FFs in Ref. [135], which gives results similar to an earlier calculation based on a zero-range model [147], and in Ref. [140]. Similar calculations could be performed for helium and triton. Unfortunately, however, pions become non-perturbative at momenta $Q \sim F_\pi$ [148] and thus this approach will fail for sufficiently dense nuclei. Much work has been done with nonperturbative pions following Refs. [66–68], as reviewed for example in Refs. [39,40]. By now, good potentials exist at N²LO and N³LO (for example, Ref. [149]), but for only narrow ranges of UV regulators. Although not consistent from an EFT perspective because they lack the necessary counterterms at each order and generate amplitudes that are not properly renormalized [41], these potentials produce results in few-body systems that are not very different from phenomenological two-plus three-body potentials such as Av18 [150] plus UIX [151]. For a calculation of PT FFs for $A = 2, 3$ systems within this approach, see Ref. [152]. Renormalization issues with currents are discussed in Ref. [42].

In Tab. 6.2 we give a sample of the most recent evaluations of $d_{d,t,h}$ in terms of the nucleon EDMs, Eqs. (38) and (39), the pion-nucleon couplings in Eq. (24), where we bury some $\bar{\Delta}$ contributions, and the other couplings in Eq. (21). For the deuteron, the one-body contribution is given by the isoscalar nucleon EDM, $2d_0 = d_n + d_p$.² Isoscalar $\cancel{\mathcal{J}}$ potentials, generated by \bar{g}_0 and $\bar{C}_{1,2}$, vanish on the deuteron. \bar{g}_0 does contribute to d_d but only through subleading potentials involving PT isospin-breaking couplings, and through two-nucleon $\cancel{\mathcal{J}}$ currents; these contributions are small [87,136] and omitted here. The \bar{g}_1 contribution to d_d shows little dependence on V_{PT} (see also Ref. [133]), and it is about a factor of 5 smaller than the expectation in Eq. (52). $\bar{\Delta}$ enters only indirectly through \bar{g}_1 .

The situation is strikingly different for helium and triton. The one-body contributions are given mostly by, respectively, d_n and d_p .³ \bar{g}_0 and \bar{g}_1 contribute at about the same level. In particular, \bar{g}_1 contributes to the isoscalar combination $d_t + d_h$, while \bar{g}_0 to the isovector, $d_t - d_h$. There is a factor-of-2 disagreement between calculations based on the No-Core Shell Model [132,136] and on the Faddeev equation [87,134]. As for the deuteron, the EDM induced by the OPE $\cancel{\mathcal{J}}$ potential is a few times smaller than the expectation in Eq. (52). Changing V_{PT} has little effect on the contribution of \bar{g}_1 , while \bar{g}_0 is more affected. The isoscalar couplings $\bar{C}_{1,2}$ give a nonvanishing contribution to $d_t - d_h$. These operators are the most sensitive to the choice of V_{PT} and to the details of the nuclear calculation, like the choice of regulator [87,136], and more conclusive results have to wait for a more consistent approach. Still, also this

²The deviation of the proportionality factor from 1 seen in Table 6.2 for the Av18 and N²LO potentials stems solely from the deuteron D -state probability P_D . However, P_D is not an observable [153], indicating that the $\sim 10\%$ difference between these potentials and the perturbative-pion result, where P_D enters only at N²LO together with other contributions, is within the theoretical error of both approaches.

³In analogy to the isoscalar trinucleon MDM [153], one expects model-dependent contributions from the trinucleon D -state probability to $d_t + d_h$ of similar size as those from P_D to d_d , see previous footnote.

	Potential (references)	d_n	d_p	\bar{g}_0/F_π	\bar{g}_1/F_π	$\bar{C}_1 F_\pi^3$	$\bar{C}_2 F_\pi^3$	$\bar{\Delta}/F_\pi m_N$
d_d	Perturbative pion [135, 147]	1	1	—	-0.23	—	—	—
	Av18 [87, 131, 136–138]	0.91	0.91	—	-0.19	—	—	—
	N ² LO [87, 137]	0.94	0.94	—	-0.18	—	—	—
d_t	Av18 [132, 136, 138]	-0.05	0.90	0.15	-0.28	0.01	-0.02	n/a
	Av18+UIX [87, 134]	-0.05	0.90	0.07	-0.14	0.002	-0.005	0.02
	N ² LO [87]	-0.03	0.92	0.11	-0.14	0.05	-0.10	0.02
d_h	Av18 [132, 136, 138]	0.88	-0.05	-0.15	-0.28	-0.01	0.02	n/a
	Av18+UIX [87, 134]	0.88	-0.05	-0.07	-0.14	-0.002	0.005	0.02
	N ² LO [87]	0.90	-0.03	-0.11	-0.14	-0.05	0.11	0.02

Table 3: Dependence of the deuteron, triton and helion EDMs on \mathcal{X} LECs for various PT potentials. Entries are dimensionless in the first two columns and in units of $e\text{fm}$ in the remaining columns. “—” indicates very small numbers.

contribution appears to be smaller than predicted by Eq. (52). $\bar{\Delta}$ now enters explicitly through the three-nucleon \mathcal{X} force, Eq. (55), but its contribution is smaller than expected by power counting and can be neglected [87].

Table 6.2 allows us to draw more precise conclusions about the relative size of EDMs, which also qualify some of the expectations in Tab. 6.2. The expectation of relatively large light-nuclear EDMs for $\bar{\theta}$, qCEDM and LR4QOs is tampered by the small effects of the OPE \mathcal{X} potential shown in Tab. 6.2. Still, the even smaller effects from the rest of the \mathcal{X} potential leave some opportunities open:

- $\bar{\theta}$: NDA suggests that $\bar{C}_{1,2}$ and explicit $\bar{\Delta}$ effects can be neglected. Using the estimates for \bar{g}_1 in Eq. (27) and the LQCD evaluation of $d_{n,p}$ in Eq. (46),

$$d_d \simeq 0.9(d_n + d_p) - 0.2 \frac{\bar{g}_1}{F_\pi}, \quad \frac{d_t + d_h}{2} \simeq 0.9 \frac{d_n + d_p}{2} - 0.1 \frac{\bar{g}_1}{F_\pi}, \quad (56)$$

which satisfy, within large uncertainties, the NDA expectation that the deuteron EDM and the helion/triton isoscalar EDM combination receive contributions of similar size from the isoscalar nucleon EDM and \bar{g}_1 . When $d_n + d_p$ is known, from either experiment or a more precise LQCD extraction, a measurement of either d_d or $d_t + d_h$ will allow a determination of \bar{g}_1 . A value of \bar{g}_1 much larger than the estimate in Eq. (27) or a d_d much larger than d_n or d_p will point to \mathcal{X} of non- $\bar{\theta}$ origin. The helion/triton isovector combination,

$$\frac{d_t - d_h}{2} \simeq 0.9 \frac{d_p - d_n}{2} - 0.1 \frac{\bar{g}_0}{F_\pi}, \quad (57)$$

is expected to be dominated by OPE, but the smallness of \bar{g}_0 and the relative suppression of the OPE contribution conspire to enhance the importance of the one-body contribution. Nonetheless, once $d_p - d_n$ is measured, Eq. (57) allows the extraction of \bar{g}_0 , and, through Eq. (26), the determination of $\bar{\theta}$, without further nonperturbative input.

- qCEDM: As for $\bar{\theta}$, $\bar{C}_{1,2}$ and $\bar{\Delta}$ should be higher order, contributing at N²LO and N³LO respectively, so Eqs. (56) and (57) also hold. In this case, however, the couplings are not well determined. If we assume that $d_{0,1}$ are approximated by their non-analytic pieces and that $\bar{g}_0 \sim \bar{g}_1$, then d_d and $d_t + d_h$ would be dominated by \bar{g}_1 , with d_0 contributing at the 10% level. Due to the logarithmic enhancement in $d_p - d_n$ and the relative suppression of OPE in $d_{t,h}$, the one-body and OPE contributions to $d_t - d_h$ should be roughly of the same size. Obviously, this is not a firm conclusion and a better grip on $d_{n,p}$ and $\bar{g}_{0,1}$ is needed from LQCD.
- LR4QOs: Similar considerations hold, except that the coupling \bar{g}_0 should be small and only d_d and $d_t + d_h$ could be enhanced with respect to $d_{n,p}$.
- gCEDM and PS4QOs: The short-range contributions from $\bar{C}_{1,2}$ are expected to be as important as the one-body contribution and OPE, but for the systems considered here the effects of the \mathcal{Z} potential are numerically smaller than expected, although highly dependent on the short-distance treatment of V_{PT} . If this result stands, Eqs. (56) and (57) hold again and also in this case LQCD input is sorely needed.
- qEDM: the simplest and most predictive situation, in which all EDMs should be well approximated by one-body contributions, and both $\bar{g}_{0,1}$ can be dropped in Eqs. (56) and (57).

Our discussion has underlined how the EDMs of light nuclei complement the nucleon EDM, and can play an important role in singling out the microscopic source of \mathcal{Z} —for specific BSM examples, see Ref. [154]. Qualitatively, EDMs of nuclei with $N = Z$ are particularly interesting: an observation in these systems of a large EDM, compared to the nucleon EDM, would suggest that \mathcal{Z} does not come from $\bar{\theta}$, but rather from isospin-breaking sources, like qCEDM or LR4QOs. Quantitative conclusions require more precise evaluations of the couplings in Eq. (21), a program under way using LQCD.

7 Outlook

We reviewed here the main steps that link \mathcal{Z} in the SM and beyond to observables where dramatic experimental progress is expected, nucleon and light-nuclear EDMs. The key idea is that EFTs enable us to keep track of symmetries across scales, with minimal assumptions about unknown dynamics. As a consequence, the various spin, isospin, and spatial profiles of light nuclei probe different aspects of (B)SM \mathcal{Z} , and various (admittedly difficult) precision measurements would allow precious information on physics at a scale comparable, or perhaps beyond, what can be reached in the energy frontier.

We sketched this link in broad terms, with an emphasis on progress over the last five-ten years. Although the framework is in place, we emphasized a few of the aspects where gaps remain. Perhaps the most pressing are *i)* a more systematic assessment of the effects of flavor-changing operators in the running of the more relevant light-quark operators; *ii)* LQCD calculations of the LECs of the \mathcal{Z} Lagrangian, either directly or making use of chiral symmetry

to relate \mathcal{J} matrix elements to T quantities; and *iii*) a fully consistent EFT treatment of the PT dynamics in nuclei beyond the deuteron.

The usefulness of this framework does not hinge solely on experiments on light nuclei. Atomic and molecular EDMs (in particular, from diamagnetic atoms) also depend to some extent on nuclear \mathcal{J} (especially Schiff moments), albeit for much heavier nuclei than we have discussed here. From the nuclear physics perspective, here lies the most important challenge: to extend the EFT approach beyond light nuclei. The last decade has witnessed extraordinary progress in the development of the so-called *ab initio* methods, which aim to calculate the properties of medium-mass nuclei starting from given internucleon forces. Most of this work, just like the trinucleon calculations presented here, treats the input, whether inspired by EFT or not, as a phenomenological potential where there is no hierarchy of interactions. With such a hybrid approach, the \mathcal{J} properties of other nuclei could certainly be calculated using as input not only a PT potential inspired by EFT, but also the \mathcal{J} interactions in Eq. (21). This would be an alternative to existing calculations (reviewed, for example, in Ref. [43]) which are typically based on three nonderivative pion-nucleon couplings and uncontrolled (but perhaps valid) approximations, such as random-phase or mean-field. We hope this review serves to stimulate such alternative calculations.

On a longer time scale, a fully consistent EFT formulation for larger nuclei would be desirable. From an *ab initio* perspective, nuclear EFT interactions cannot be treated as a black box, but instead subleading interactions should be included in perturbation theory to avoid extraneous regulator dependence. From a more effective perspective, an in-medium EFT appropriate for heavy nuclei should be formulated. The many regularities found among nuclear properties offer great opportunities for the effective field theorist.

Acknowledgments

Our understanding of \mathcal{J} benefited tremendously from the insights of our collaborators V. Cirigliano, J. de Vries, J. Engel, R. Higa, W. Hockings, C.-P. Liu, C. Maekawa, M. Ramsey-Musolf, I. Stetcu, R. Timmermans and A. Walker-Loud. We thank J. de Vries for comments on the manuscript, and T. Blum, T. Izubuchi, E. Shintani and B. Yoon for providing us with LQCD results and for interesting discussions. The research of EM was supported by the LDRD program at Los Alamos National Laboratory. This material is based upon work supported in part by the U.S. Department of Energy, Office of Science, Office of Nuclear Physics, under Award Number DE-FG02-04ER41338.

References

- [1] Sakharov A. *Pisma Zh.Eksp.Teor.Fiz.* 5:32 (1967)
- [2] Steigman G. *Ann.Rev.Astron.Astrophys.* 14:339 (1976)
- [3] Weinberg S. *Phys.Rev.Lett.* 19:1264 (1967)
- [4] Salam A. *Conf.Proc.* C680519:367 (1968)

- [5] Kobayashi M, Maskawa T. *Prog.Theor.Phys.* 49:652 (1973)
- [6] Jarlskog C. *Phys.Rev.Lett.* 55:1039 (1985)
- [7] Olive K, et al. *Chin.Phys.* C38:090001 (2014)
- [8] Canetti L, Drewes M, Shaposhnikov M. *New J.Phys.* 14:095012 (2012)
- [9] Baker C, et al. *Phys.Rev.Lett.* 97:131801 (2006)
- [10] Kumar K, Lu ZT, Ramsey-Musolf MJ arXiv:1312.5416 [hep-ph] (2013)
- [11] Pospelov M, Ritz A. *Annals Phys.* 318:119 (2005)
- [12] Seng CY. *Phys.Rev.* C91:025502 (2015)
- [13] Semertzidis YK arXiv:1110.3378 [physics.acc-ph] (2011)
- [14] Pretz J. *Hyperfine Interact.* 214:111 (2013)
- [15] Bennett G, et al. *Phys.Rev.* D80:052008 (2009)
- [16] 't Hooft G. *Phys.Rev.Lett.* 37:8 (1976)
- [17] Peccei R, Quinn HR. *Phys.Rev.Lett.* 38:1440 (1977)
- [18] Weinberg S. *Phys.Rev.Lett.* 40:223 (1978)
- [19] Wilczek F. *Phys.Rev.Lett.* 40:279 (1978)
- [20] Weinberg S. *Phys.Rev.Lett.* 43:1566 (1979)
- [21] Bilenky SM, Giunti C. *Int.J.Mod.Phys.* A30:1530001 (2015)
- [22] Bilenky SM, Hosek J, Petcov S. *Phys.Lett.* B94:495 (1980)
- [23] Fukugita M, Yanagida T. *Phys.Lett.* B174:45 (1986)
- [24] Buchmuller W, Wyler D. *Nucl.Phys.* B268:621 (1986)
- [25] Grzadkowski B, Iskrzynski M, Misiak M, Rosiek J. *JHEP* 1010:085 (2010)
- [26] De Rujula A, Gavela M, Pene O, Vegas F. *Nucl.Phys.* B357:311 (1991)
- [27] Weinberg S. *Phys.Rev.Lett.* 63:2333 (1989)
- [28] Ramsey-Musolf M, Su S. *Phys.Rept.* 456:1 (2008)
- [29] Ng J, Tulin S. *Phys.Rev.* D85:033001 (2012)
- [30] Bedaque PF, van Kolck U. *Ann.Rev.Nucl.Part.Sci.* 52:339 (2002)

- [31] Baluni V. *Phys.Rev.* D19:2227 (1979)
- [32] Crewther R, Di Vecchia P, Veneziano G, Witten E. *Phys.Lett.* B88:123 (1979)
- [33] Mereghetti E, Hockings W, van Kolck U. *Annals Phys.* 325:2363 (2010)
- [34] Maekawa C, Mereghetti E, de Vries J, van Kolck U. *Nucl.Phys.* A872:117 (2011)
- [35] de Vries J, Mereghetti E, Timmermans R, van Kolck U. *Annals Phys.* 338:50 (2013)
- [36] Bsaisou J, Meissner UG, Nogga A, Wirzba A arXiv:1412.5471 [hep-ph] (2014)
- [37] Dekens W, de Vries J. *JHEP* 1305:149 (2013)
- [38] Barnea N, et al. *Phys.Rev.Lett.* 114:052501 (2015)
- [39] Machleidt R, Entem D. *Phys.Rept.* 503:1 (2011)
- [40] Epelbaum E, Meissner UG. *Ann.Rev.Nucl.Part.Sci.* 62:159 (2012)
- [41] Nogga A, Timmermans R, van Kolck U. *Phys.Rev.* C72:054006 (2005)
- [42] Pavón Valderrama M, Phillips DR. *Phys.Rev.Lett.* 114:082502 (2015)
- [43] Engel J, Ramsey-Musolf MJ, van Kolck U. *Prog.Part.Nucl.Phys.* 71:21 (2013)
- [44] Manohar AV, Wise MB. *Phys.Lett.* B636:107 (2006)
- [45] Alonso R, Jenkins EE, Manohar AV, Trott M. *JHEP* 1404:159 (2014)
- [46] Brod J, Haisch U, Zupan J. *JHEP* 1311:180 (2013)
- [47] Kagan AL, et al. *Phys.Rev.Lett.* 114:101802 (2015)
- [48] Isidori G, Kamenik JF, Ligeti Z, Perez G. *Phys.Lett.* B711:46 (2012)
- [49] Sala F. *JHEP* 1403:061 (2014)
- [50] Hagiwara K, Peccei R, Zeppenfeld D, Hikasa K. *Nucl.Phys.* B282:253 (1987)
- [51] Espriu D, Tarrach R. *Z.Phys.* C16:77 (1982)
- [52] Dekens W, de Vries J (in preparation)
- [53] Braaten E, Li CS, Yuan TC. *Phys.Rev.Lett.* 64:1709 (1990)
- [54] An H, Ji X, Xu F. *JHEP* 1002:043 (2010)
- [55] Hisano J, Tsumura K, Yang MJ. *Phys.Lett.* B713:473 (2012)
- [56] Degrassi G, Franco E, Marchetti S, Silvestrini L. *JHEP* 0511:044 (2005)

- [57] Grojean C, Jenkins EE, Manohar AV, Trott M. *JHEP* 1304:016 (2013)
- [58] Chang D, Choi K, Keung WY. *Phys.Rev.* D44:2196 (1991)
- [59] Barr SM, Zee A. *Phys.Rev.Lett.* 65:21 (1990)
- [60] Kamenik JF, Papucci M, Weiler A. *Phys.Rev.* D85:071501 (2012)
- [61] Manohar A, Georgi H. *Nucl.Phys.* B234:189 (1984)
- [62] Georgi H, Randall L. *Nucl.Phys.* B276:241 (1986)
- [63] Weinberg S. *Physica* A96:327 (1979)
- [64] Gasser J, Leutwyler H. *Annals Phys.* 158:142 (1984)
- [65] Gasser J, Leutwyler H. *Nucl.Phys.* B250:465 (1985)
- [66] Weinberg S. *Phys.Lett.* B251:288 (1990)
- [67] Weinberg S. *Nucl.Phys.* B363:3 (1991)
- [68] Ordonez C, van Kolck U. *Phys.Lett.* B291:459 (1992)
- [69] Weinberg S. *Phys.Rev.* 166:1568 (1968)
- [70] Coleman SR, Wess J, Zumino B. *Phys.Rev.* 177:2239 (1969)
- [71] Callan Curtis G. J, Coleman SR, Wess J, Zumino B. *Phys.Rev.* 177:2247 (1969)
- [72] Weinberg S (1996)
- [73] van Kolck U. *Few Body Syst.Suppl.* 9:444 (1995)
- [74] Jenkins EE, Manohar AV. *Phys.Lett.* B255:558 (1991)
- [75] Pascalutsa V, Phillips DR. *Phys.Rev.* C67:055202 (2003)
- [76] Long B, van Kolck U. *Nucl.Phys.* A840:39 (2010)
- [77] Long B, van Kolck U. *Nucl.Phys.* A870-871:72 (2011)
- [78] Bijmans J, Colangelo G, Ecker G. *JHEP* 9902:020 (1999)
- [79] Fettes N, Meissner UG, Mojzis M, Steininger S. *Annals Phys.* 283:273 (2000)
- [80] Ordonez C, Ray L, van Kolck U. *Phys.Rev.* C53:2086 (1996)
- [81] van Kolck U. *Phys.Rev.* C49:2932 (1994)
- [82] Cheng HY. *Phys.Rev.* D44:166 (1991)

- [83] Pich A, de Rafael E. *Nucl.Phys.* B367:313 (1991)
- [84] Cho PL. *Phys.Rev.* D48:3304 (1993)
- [85] Borasoy B. *Phys.Rev.* D61:114017 (2000)
- [86] Cheng HY. *Chin.J.Phys.* 49:580 (2011)
- [87] Bsaisou J, et al. *JHEP* 1503:104 (2015)
- [88] Aoki S, et al. *Eur.Phys.J.* C74:2890 (2014)
- [89] Walker-Loud A. *PoS LATTICE2013*:013 (2014)
- [90] Borsanyi S, et al. *Science* 347:1452 (2015)
- [91] Bali G, et al. *Nucl.Phys.* B866:1 (2013)
- [92] Amoros G, Bijmans J, Talavera P. *Nucl.Phys.* B602:87 (2001)
- [93] Hoferichter M, Kubis B, Meiner UG. *Nucl.Phys.* A833:18 (2010)
- [94] Pospelov M. *Phys.Lett.* B530:123 (2002)
- [95] Walker-Loud A. *private communication* (2014)
- [96] Barton G. *Nuovo Cim.* 19:512 (1961)
- [97] Georgi H, Kaplan DB, Randall L. *Phys.Lett.* B169:73 (1986)
- [98] Thomas SD. *Phys.Rev.* D51:3955 (1995)
- [99] Hockings W, van Kolck U. *Phys.Lett.* B605:273 (2005)
- [100] Narison S. *Phys.Lett.* B666:455 (2008)
- [101] Ottnad K, Kubis B, Meissner UG, Guo FK. *Phys.Lett.* B687:42 (2010)
- [102] Mereghetti E, et al. *Phys.Lett.* B696:97 (2011)
- [103] de Vries J, Timmermans R, Mereghetti E, van Kolck U. *Phys.Lett.* B695:268 (2011)
- [104] Schiff L. *Phys.Rev.* 132:2194 (1963)
- [105] O'Connell D, Savage MJ. *Phys.Lett.* B633:319 (2006)
- [106] Guo FK, Meissner UG. *JHEP* 1212:097 (2012)
- [107] Akan T, Guo FK, Meiner UG. *Phys.Lett.* B736:163 (2014)
- [108] Bernard V, Kaiser N, Meissner UG. *Int.J.Mod.Phys.* E4:193 (1995)

- [109] Maekawa C, van Kolck U. *Phys.Lett.* B478:73 (2000)
- [110] Maekawa C, Veiga J, van Kolck U. *Phys.Lett.* B488:167 (2000)
- [111] He XG, McKellar BH, Pakvasa S. *Int.J.Mod.Phys.* A4:5011 (1989)
- [112] Seng CY, et al. *Phys.Lett.* B736:147 (2014)
- [113] Lin HW. *AIP Conf.Proc.* 1441:540 (2012)
- [114] Shintani E, Blum T, Soni A, Izubuchi T. *PoS LATTICE2013*:298 (2014)
- [115] Guo FK, et al. arXiv:1502.02295 [hep-lat] (2015)
- [116] Shintani E. *private communication* (2015)
- [117] Pospelov M, Ritz A. *Nucl.Phys.* B573:177 (2000)
- [118] Pospelov M, Ritz A. *Phys.Rev.Lett.* 83:2526 (1999)
- [119] Hisano J, Lee JY, Nagata N, Shimizu Y. *Phys.Rev.* D85:114044 (2012)
- [120] Pospelov M, Ritz A. *Phys.Rev.* D63:073015 (2001)
- [121] Bhattacharya T, et al. (in preparation)
- [122] Gupta R, et al. *PoS Lattice2014*:152 (2014)
- [123] Bhattacharya T, Gupta R, Yoon B arXiv:1503.05975 [hep-lat] (2015)
- [124] Bacchetta A, Courtoy A, Radici M. *JHEP* 1303:119 (2013)
- [125] Anselmino M, et al. *Phys.Rev.* D87:094019 (2013)
- [126] Bhattacharya T, et al. arXiv:1502.07325 [hep-ph] (2015)
- [127] Donoghue JF, Holstein BR, Borasoy B. *Phys.Rev.* D59:036002 (1999)
- [128] de Vries J, Mereghetti E, Walker-Loud A (in preparation)
- [129] Fuyuto K, Hisano J, Nagata N. *Phys.Rev.* D87:054018 (2013)
- [130] Lebedev O, Olive KA, Pospelov M, Ritz A. *Phys.Rev.* D70:016003 (2004)
- [131] Liu CP, Timmermans R. *Phys.Rev.* C70:055501 (2004)
- [132] Stetcu I, et al. *Phys.Lett.* B665:168 (2008)
- [133] Afnan I, Gibson B. *Phys.Rev.* C82:064002 (2010)
- [134] Song YH, Lazauskas R, Gudkov V. *Phys.Rev.* C87:015501 (2013)

- [135] de Vries J, Mereghetti E, Timmermans R, van Kolck U. *Phys.Rev.Lett.* 107:091804 (2011)
- [136] de Vries J, et al. *Phys.Rev.* C84:065501 (2011)
- [137] Bsaisou J, et al. *Eur.Phys.J.* A49:31 (2013)
- [138] Yamanaka N, Hiyama E arXiv:1503.04446 [nucl-th] (2015)
- [139] Liu CP, et al. *Phys.Lett.* B713:447 (2012)
- [140] Mereghetti E, de Vries J, Timmermans R, van Kolck U. *Phys.Rev.* C88:034001 (2013)
- [141] Liu CP, Timmermans R. *Phys.Lett.* B634:488 (2006)
- [142] Song YH, Lazauskas R, Gudkov V. *Phys.Rev.* C83:065503 (2011)
- [143] Haxton W, Henley E. *Phys.Rev.Lett.* 51:1937 (1983)
- [144] Kaplan DB, Savage MJ, Wise MB. *Nucl.Phys.* B534:329 (1998)
- [145] Kaplan DB, Savage MJ, Wise MB. *Phys.Rev.* C59:617 (1999)
- [146] Savage MJ, Springer RP. *Nucl.Phys.* A686:413 (2001)
- [147] Khriplovich I, Korkin R. *Nucl.Phys.* A665:365 (2000)
- [148] Fleming S, Mehen T, Stewart IW. *Nucl.Phys.* A677:313 (2000)
- [149] Epelbaum E, Glockle W, Meissner UG. *Nucl.Phys.* A747:362 (2005)
- [150] Wiringa RB, Stoks V, Schiavilla R. *Phys.Rev.* C51:38 (1995)
- [151] Pudliner B, et al. *Phys.Rev.* C56:1720 (1997)
- [152] Piarulli M, et al. *Phys.Rev.* C87:014006 (2013)
- [153] Friar JL. *Phys.Rev.* C20:325 (1979)
- [154] Dekens W, et al. *JHEP* 1407:069 (2014)